Shallow Water Waves and Boundary Effects

Erik Simonsen

Norwegian University of Life Sciences
Department of mathematical sciences and technology
Master Thesis 30 credits 2013

Preface

This thesis marks the end of my master's degree in Environmental Physics and Renewable Energy at the University of Life Sciences, UMB.

A big thank you to my supervisor at UMB, Professor Peder Tyvand, for meeting me weekly and sharing your ideas. Your insight in fluid mechanics is truly inspiring.

The master thesis is written in cooperation with Nexans Norway AS. In that occasion, I would like to express my gratitude to Jon Steinar Andreassen, Inge Vintermyr and Kjetil-André Karlsen at Nexans Norway AS. Thank you for your guidance and for giving me the opportunity to write my master thesis in cooperation with a leading engineering company.

Finally, I would like to thank my parents, Turid and Pål, my brother Andreas and my girlfriend Martine for all the support and encouragement throughout my academic career.

Ås, 10.05.2013

_____

Erik Simonsen

Abstract

This thesis is written in cooperation with Nexans Norway AS and evaluates wave theories applied in calculations of wave loads on submarine structures. Nexans Norway AS has provided metocean and soil data from an on-going British Petroleum project outside the coast of Egypt that is used as a case study.

This thesis aim to investigate the range of validity for the linear Airy theory in shallow and transitional waters. The Airy theory is a simple and frequently used wave theory in coastal engineering to approximate the wave kinematics. To evaluate the Airy theory's validity and accuracy in shallow and transitional water depths, the theory is used to calculate the particle velocity 0.5 meter above seabed in these water depths.

Stokes 2nd order wave theory is a non-linear expansion of the Airy theory and is also included in the calculations. The results from both wave theories are evaluated and compared with results from the numerical stream function theory.

The results of the particle velocity calculations indicate significant differences between the Airy theory and the stream function theory for shallow and transitional water depths. Stokes 2nd order wave theory provides overall better results than the Airy theory in comparison with the results from the stream function theory, especially for the shallowest water depths included in the study.

A research study of boundary layer effects close to the seabed is carried out in the thesis. Stokes oscillating boundary layer theory is described in detail and equations from the theory is derived with variable viscosity. Padé approximants are used to approximate the variable viscosity function. The results indicate that the boundary layer affects the velocity profile. The boundary layer thickness is shown to increase with increasing viscosity.

In this thesis, only an introduction to sediment transport theory is carried out. To get a full evaluation of the boundary layer effects on the wave flow, further work is recommended to include sediment transport in the calculations wave flow in the boundary layer.

Sammendrag

Denne masteroppgaven er skrevet i samarbeid med Nexans Norway AS og undersøker bølgeteorier brukt til å bestemme belastningen fra havbølger på undersjøiske konstruksjoner. Nexans Norway AS har fremlagt bølge- og havbunnsdata fra et pågående British Petroleum prosjekt utenfor Egypt som vil bli brukt i beregningene i denne oppgaven.

Masteroppgaven tar sikte på å undersøke gyldighetsområde til Airy-teorien i grunt og mellom-grunt vann. Den lineære Airy-teorien er en enkel og mye brukt bølgeteori for å approksimere havbølgers kinematikk. For å undersøke Airy-teoriens nøyaktighet på grunt og mellom-grunt vann, skal partikkelhastigheten til bølgestrømningen 0.5 meter over havbunnen beregnes i disse vanndybdene. Stokes 2. ordens bølgeteori er en ikke-lineær utvikling av Airy-teorien og vil også være inkludert i beregningene. Resultatene fra begge teoriene vil bli undersøkt og sammenliknet med resultater fra den numeriske strømfunksjonsteorien.

Resultatene indikerer signifikante forskjeller mellom Airy-teorien og strømfunksjonsteorien i beregningene av partikkelhastighetene på grunt og mellom-grunt vann. Stokes 2. ordens teori gir generelt bedre resultater enn Airy-teorien i sammenlikning med resultatene fra strømfunksjonsteorien. Dette gjelder spesielt på de grunneste vanndybdene inkludert i undersøkelsene.

En litteraturstudie av grensesjikteffekter på strømningen nær sjøbunnen er inkludert i masteroppgaven. Stokes oscillatoriske grensesjiktteori blir beskrevet i detalj og ligninger fra denne teorien blir utledet med variabel viskositet. Padé-approksimasjon blir brukt for å approksimere den variable viskositetsfunksjonen. Resultatene indikerer at hastighetsprofilen blir påvirket i grensesjiktet. Grensesjikttykkelsen blir vist til å øke ved økning i viskositeten.

Masteroppgaven gir en kort introduksjon i sedimenttransport-teori. For en fullstendig evaluering av grensesjikteffekter, anbefales videre arbeid å inkludere sedimenttransport i beregninger av bølgestrømningen i grensesjiktet.

Table of contents

List of figures

List of tables

Acronyms

BBC – Bottom Boundary Condition

DNV – Det Norske Veritas

DFSBC – Dynamic Free Surface Boundary Condition

KFSBC – Kinematic Free Surface Boundary Condition

Metocean – Metrological and oceanographic

RP – Recommended Practice

SWL – Still water level

1. Introduction

This master thesis is written in cooperation with Nexans Norway AS. Nexans Norway AS develops, manufactures and markets submarine cables [1]. In developing, designing and manufacturing submarine cables for new locations, accurate calculations of environmental loads are a crucial. Loads from waves and current can in the worst case scenario cause structural damages, fatigue and cable instability.

1.1 Objectives

The wave load in shallow and transitional waters is of interest in this thesis. Chapter 2 describes the basic principles in water wave theory and a detailed description of the wave theories that will be applied to the case study provided by Nexans Norway AS. In engineering applications, the Airy theory is a commonly used wave theory to approximate the wave kinematics. The Airy theory is easy to use and provides in general good estimates of the wave kinematics when the wave height is much smaller than the water depth. This is not the case in shallow and transitional waters. Therefore, an evaluation of the Airy theory's validity in shallow and transitional waters will be done. The results of the particle velocity 0.5 meter above seabed for different water depths will be compared with results obtained by using the numerical stream function theory.

In chapter 3, boundary layer theory is described. Just above the seabed, shear stress in the boundary layer may influence the wave flow. Therefore, a research study of boundary layer effects on the wave flow is carried out to investigate if and how the boundary layer affects the horizontal velocity just above the seabed.

1.2 Metocean and soil data

Nexans Norway AS has provided the metrological and oceanographic (metocean) data applied in this thesis. The data is extracted from the on-going BP umbilical study named "West Nile Delta" outside the coast of Egypt. An overview of the West Nile Delta field is shown in Figure 1. Table 1 contains the omni-directional 100 year return period wave data that has been extracted for water depth range between 10 and 50 m. The wave data is applicable from shore and towards Raven PLEM, illustrated in Figure 1. The regular wave properties from Table 1 will be applied in the calculations of the wave kinematics.

Water depth	Direction	Irregular wave properties			Regular wave properties	
		Hs	Tz	Tp	Hmax	THmax
[m]	[From]	[m]	[s]	[s]	[m]	[s]
10	Omni-Directional	3.6	6.7	12.6	7	12.7
15	Omni-Directional	5.9	8.4	13.9	11.5	14
25	Omni-Directional	7.5	9.3	14.5	14.4	14.6
35	Omni-Directional	7.6	9.2	13.9	14.5	14
50	Omni-Directional	7.6	NA	14	14.3	14.1

Table 1: Metocean data for the West Nile Delta.

The soil data for the seabed at the West Nile Delta is listed in Table 2. The seabed consists of silty sand with measured median grain size *d50* and calculated roughness Z_0.

Soil type	Depth range	Grain size d50	Roughness Z_0	Submerged unit soil weight
	[m]	[mm]	[m]	[N/m^3]
Silty sand	0-1.8	0.0625	5.21E-06	8500

Table 2: Soil data.

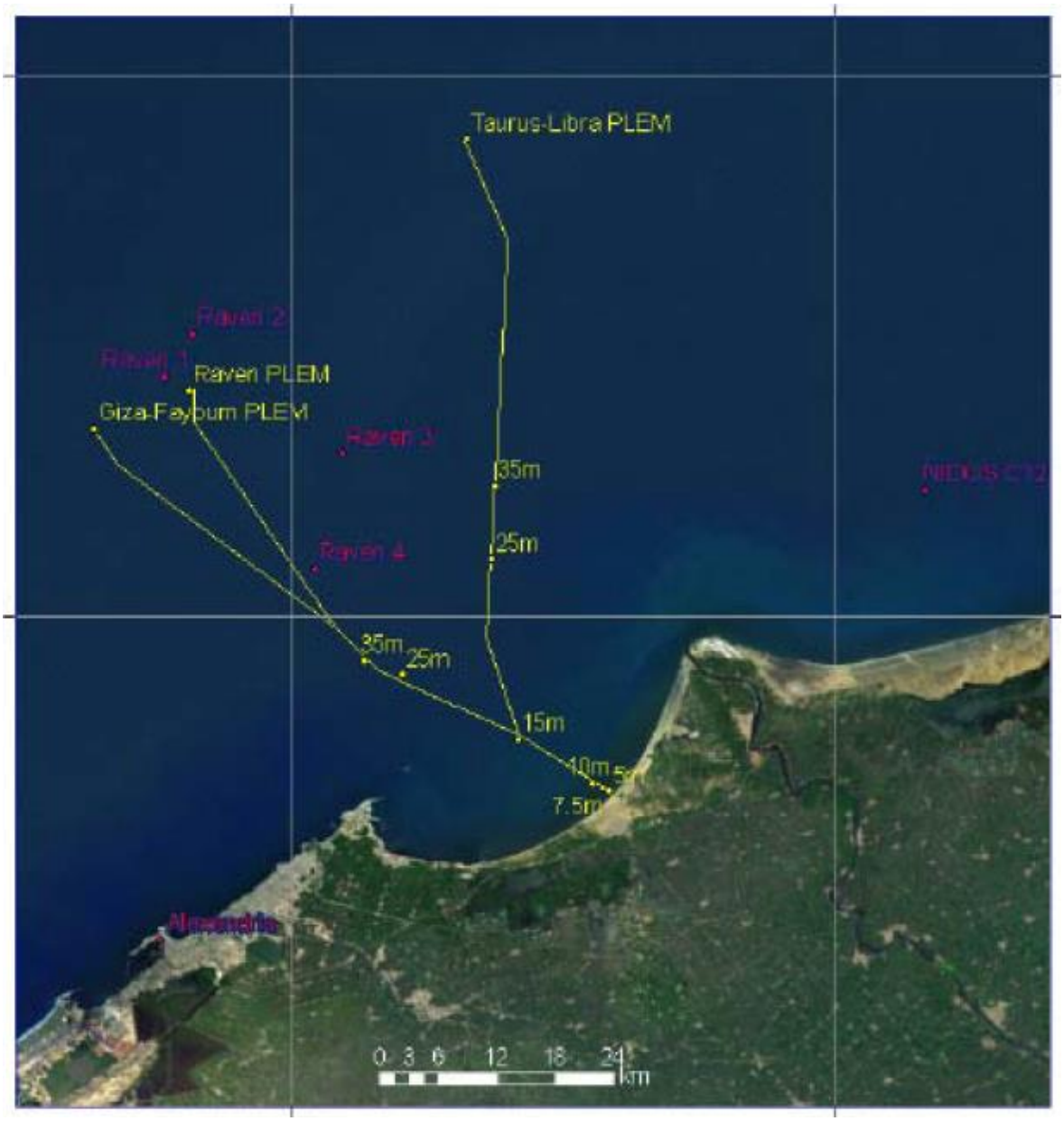

Figure 1: West Nile Delta field outside the coast of Egypt.

2. Wave theory

2.1 General

A wave can be described as a signal that propagates from one medium to another with a characteristic velocity. The signal can change properties like velocity, direction and size, and still be recognized. Waves can take form in fluids, gasses and vacuum, and these waves share common characteristics and can be examined with the same general wave theory [2].

Wave motion can operate as a single pulse or in periodic motion, called wave trains. The wavelength λ for a wave is defined as the distance between two successive crests. The waves are oscillating through the still water level (SWL) with a height called amplitude. The wave height is the distance from the wave trough to the wave crest and is twice the amplitude for linear waves. Figure 2 illustrates the terminology used in wave theory.

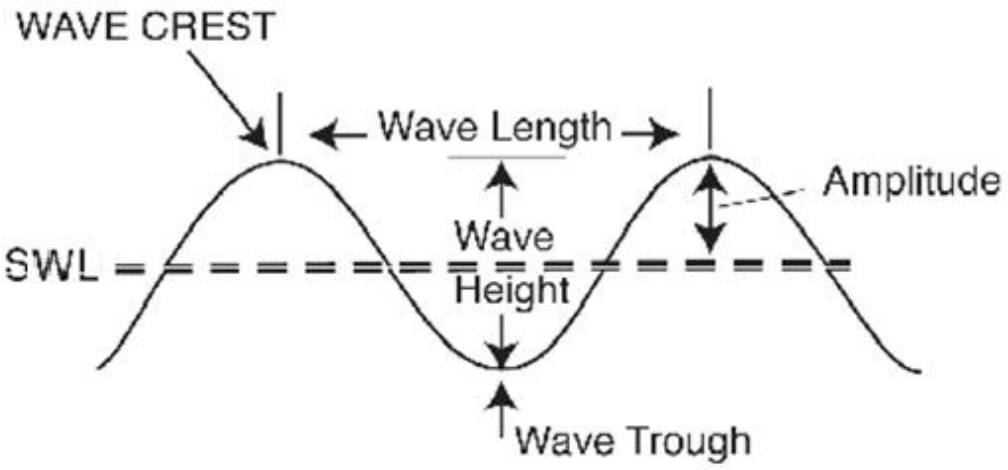

Figure 2: Illustration of terminology used to describe waves [3].

The wave period T is the time interval that two successive crests use to pass a specified point. The relation between wavelength λ and wave period T gives the following expression for the phase velocity c

$$c = \frac{\lambda}{T} \qquad (1)$$

Other characteristic wave parameters are the angular velocity ω and the wave number k

$$\omega = \frac{2\pi}{T} \tag{2}$$

$$k = \frac{2\pi}{\lambda} \tag{3}$$

where T is the wave period and λ is the wavelength.

2.1.2 Ocean waves

Ocean waves are highly irregular wave trains, which mean that the wave height, wavelength and direction of propagation vary unpredictably. Irregular waves can be analysed by summing up many simple, regular waves as shown in Figure 3. This concept is known as the superposition principle [4].

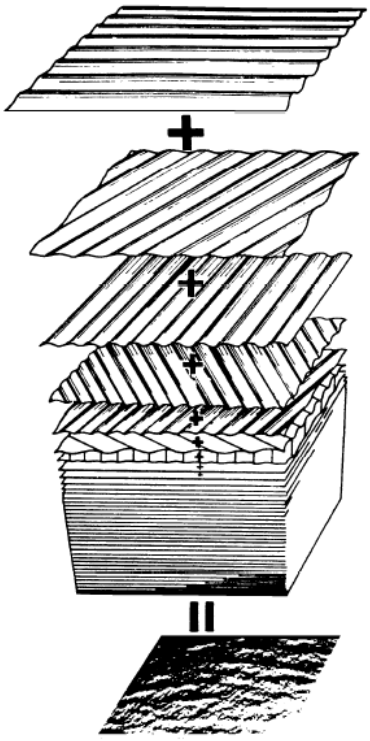

Figure 3: Concept behind the superposition principle [4].

Ocean waves consist of several different wave types which have different caused of propagation, such as surface waves, internal waves and inertial waves [5].

Surface waves

Surface waves are caused by external forces which add energy to the waves. These external forces originate mainly from wind effects, but effects from tides, moving vessels and seismic disturbance from the seabed can also occur. The energy is transmitted across the surface, causing oscillating water motion. The oscillating water motion is continuous due to gravitational and inertial forces and wave formation occurs. Surface waves caused by wind have a wave period between 1 to 30 s [6], which is applicable for the West Nile Delta case.

Internal and inertial waves

Internal waves are associated with the balance of kinetic and potential energy due to density differences beneath the sharp interface with the atmosphere. The density differences in seawater are small, which results in low frequency waves. Internal waves have a period on the order of minutes and the effect of internal waves is generally negligible in ocean engineering [5].

Inertial waves are caused by the Coriolis effect and tides. These waves have even lower frequency than internal waves and could by the same argument as for internal waves be neglected in ocean engineering [5].

2.1.3 Wave statistics

Waves are usually measured at a fixed point over a specific time interval. The surface elevation is most often recorded, but wave direction can also be analysed with sophisticated instruments [4]. It is the irregular wave properties that are measured, and statistics is used to derive the regular wave properties that are used in the calculations in this thesis. The regular wave period T is found from the measured zero up-crossing period and peak period. The regular wave height is derived from the significant wave height, which is defined as the average of the 1/3 highest waves recorded [4].

2.2 Airy theory – Linear wave theory

Airy theory is the simplest and most used wave theory. The theory is a 1st order wave theory, also known as small-amplitude or linear wave theory. The named Airy is derived from the theory's developer, the British mathematician and astronomer George B. Airy, which presented the theory in 1845 [7]. Despite of the theory's simplicity, the Airy theory has shown to give useful approximations of kinematic and dynamic properties of surface waves. In engineering applications, the Airy theory is often used in first approximation of wave behaviour [6; 8].

Assumptions

To obtain its simplicity, the Airy theory makes several assumptions. The wave motion is assumed to be periodic, freely propagating and in two dimensions [6].

The wave height H is assumed to be much smaller than the wavelength λ and the water depth d, thereby the name small-amplitude theory [6]. This assumption limits the Airy theory for high waves in transitional and shallow waters.

The water is assumed to be homogeneous, incompressible and inviscid [8]. The surface tension effects can also be neglected, due to much longer wavelength than 3 cm where surface tension effects are important [6].

The flow is assumed to be irrotational, thus shear stress at the seabed and at the surface is neglected. External forces from wind and current are also being neglected. The surface pressure on the air-sea interface is assumed to be uniform [6].

The last assumption is concerning the seabed, which is assumed to be horizontal and impermeable [8].

Velocity potential

The velocity potential is a function dependent on the wave height *H,* wave depth *d,* wave period *T,* spatial position *x* and *z* and time *t.* By the assumptions of irrotational flow and ideal fluid, the governing equation for the velocity potential Φ in Airy theory is the Laplace equation [9]

$$\frac{\partial^2 \Phi}{\partial x^2} + \frac{\partial^2 \Phi}{\partial z^2} = 0 \tag{4}$$

where *x* and *z* is respectively the horizontal and vertical coordinate.

Newman computes in [5] the following expression for the velocity potential Φ for linear waves at finite depth

$$\Phi = \frac{gH}{2\omega} \frac{\cosh k(d+z)}{\cosh kd} sin(kx - \omega t) \tag{5}$$

where g is the acceleration of gravity, *H is the* wave height, ω is the angular velocity, k is the wave number, d is the water depth, z is the vertical coordinate referenced to the SWL and positive upwards, x horizontal coordinate and t is time.

The dispersion relation in terms of angular frequency ω and the wave number k is expressed by [5]

$$\omega^2 = gk \tanh kd \tag{6}$$

where g is the acceleration of gravity and d is the water depth.

Surface elevation

Sorensen derives in [6] the following expression for the surface elevation η using the dynamic boundary condition with $z = 0$ in equation (5) and inserting the dispersion relation in (6)

$$\eta = \frac{H}{2} cos(kx - \omega t) \tag{7}$$

where *H is the* wave height, *k* is the wave number, *x* is the horizontal coordinate, ω is the angular velocity and *t* is time.

It follows from equation (7) that Air theory describes oscillating waves that are symmetric around the still water level (SWL).

Particle velocity

An important part of the on-bottom stability analysis is to calculate the environmental loads from waves on marine structures [10]. In order to calculate wave loads, the particle velocity needs to be determined. Expressed by the velocity potential Φ, the horizontal particle velocity *u* and the vertical particle velocity *w* is defined as [6]

$$u = \frac{\partial \Phi}{\partial x} \tag{8}$$

$$w = \frac{\partial \Phi}{\partial z} \tag{9}$$

where *x and z* is respectively the horizontal coordinate and the vertical coordinate referenced to the SWL and positive upwards.

By inserting equation (5) and the dispersion relation in (6) in equation (8) and (9), gives the following expression for respectively the horizontal and vertical particle velocity *u* and *w* [6]

$$u = \frac{\pi H}{T} \frac{cosh\, k(d+z)}{sinh\, kd} cos(kx - \omega t) \tag{10}$$

$$w = \frac{\pi H}{T} \frac{sinh\, k(d+z)}{sinh\, kd} cos(kx - \omega t) \tag{11}$$

where *H is the* wave height, *T* is the wave period, *k* is the wave number, *d* is the water depth, *z* is the distance below the SWL, *x* horizontal coordinate, ω is the angular velocity and *t* is time.

Notice that either spatial position *x* or the time *t* is held fixed in calculations of surface elevation in equation (7) and particle velocity in equation (10) and (11). Usually in engineering applications and in this thesis, the time history is of interest. Therefore, the spatial position *x* is held fixed.

Hence equation (10) and (11), the horizontal particle velocity *u* and the vertical particle velocity *w* have a phase difference of a quarter period and different magnitude. This relation results in elliptical particle motion [5], as seen in Figure 4. At the seabed, the particles motion is completely horizontal, following a reversing path.

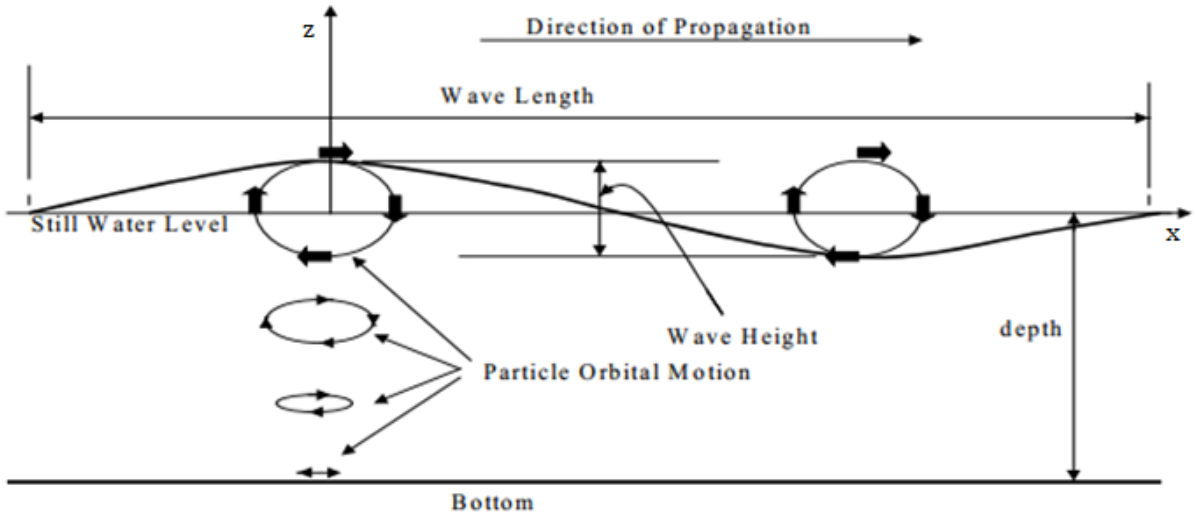

Figure 4: Illustration of the development of particle motion in a wave from the seabed to the surface [11].

2.2.1 DNV-RP-C205

Det Norske Veritas (DNV) is an independent foundation that works with risk assessment for different industry areas, especially the maritime industry [12]. In October 2010, DNV released an updated version of their recommended practice for environmental conditions and environmental loads, called DNV-RP-C205. DNV-RP-C205 gives guidance for calculations of environmental loads from waves, wind, current and tides on

submarine structures. The wave section covers linear and several non-linear wave theories, and the applicability for the different wave theories [10].

Intermediate Airy wave theory – Approximation of particle velocity

In intermediate Airy wave theory, linear wave theory is applied on waves in water depths that are in the transitional layer between deep and shallow water. As mention previously, metocean data for a specific site usually contains water depth *d,* wave height *H* and wave period *T*. To approximate the wavelength λ, DNV-RP-C205 [10] uses the following formula

$$\lambda = T(gd)^{1/2}\left(\frac{f(\varpi)}{1+\varpi f(\varpi)}\right)^{1/2} \tag{12}$$

with

$$f(\varpi) = 1 + \sum_{n=1}^{4} \alpha_n \varpi^n \tag{13}$$

$$\varpi = \frac{4\pi^2 d}{gT^2} \tag{14}$$

$$\alpha_1 = 0.666 \quad \alpha_2 = 0.445 \quad \alpha_3 = -0{,}105 \quad \alpha_4 = 0.272$$

where *T* is the wave period, *g* is the acceleration of gravity and *d* is the water depth.

The approximated wavelength is used to calculate the wave number *k*, given in equation (3). The amount of information is now sufficient to calculate the horizontal particle velocity *u* and vertical particle velocity *w* using respectively equation (10) and equation (11).

2.3 Range of validity for different wave theories

In DNV-RP-C205, the wave height H, the wave period T and the water depth d is used to determine the validity of different wave theories [13]. The following three parameters that can be extracted from metocean data are used to define respectively the wave steepness parameter S, the shallow water parameter μ and the Ursell number U_R [10]

$$S = 2\pi \frac{H}{gT^2} \tag{15}$$

$$\mu = 2\pi \frac{d}{gT^2} \tag{16}$$

$$U_R = \frac{H\lambda^2}{d^3} \tag{17}$$

where H *is the* wave height, g is the acceleration of gravity, T is the wave period, d is the water depth and λ is the wavelength.

Figure 5 is used by DNV in [10] to determine the validity of wave theories. The red points marked in Figure 5 represent, from left to right, the water depth range from 10 to 50 m at the West Nile Delta. Notice that the points are far outside the validity range for the Airy theory. Hence, the Airy theory is not expected to give good approximations of the wave kinematics at the West Nile Delta.

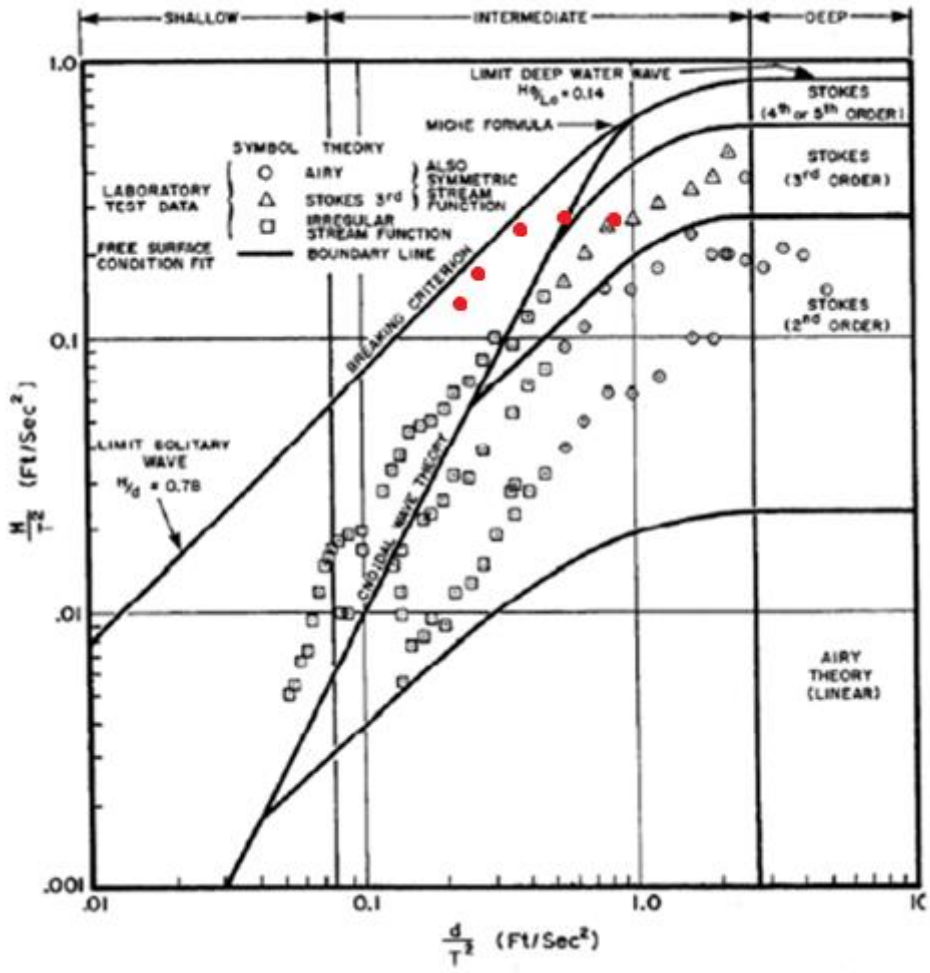

Figure 5: Ranges of validity for wave theories. The horizontal axis represents the shallowness of the water while the vertical axis represents steepness of the wave [13].

In Figure 5, the red points lie relative close to the Cnoidal wave theory line in. To check if Cnoidal wave theory is applicable, the steepness of the wave crests is examined. Cnoidal waves have sharp crests and wide troughs, with a crest to wave height ratio between 0.635 and 1. The crest height A_c and the crest to height ratio can be calculated using the following expressions [10]

$$A_C = \frac{H}{2}\left(1 + \frac{\pi H}{2\lambda}\right) \tag{18}$$

$$crest\ to\ heigt\ ratio = \frac{A_c}{H} \tag{19}$$

where H is the wave height and λ is the wavelength.

Calculations of the crest to height ratio using equation (18) and (19) give values around 0.55 for the different water depths, as shown in Table 3. This is outside the range between 0.635 and 1. Cnoidal wave theory is therefore not applicable in the West Nile Delta case [10].

Water depth [m]	**Crest to height ratio**
10	0.5456
15	0.5560
25	0.5537
35	0.5499
50	0.5432

Table 3: Crest to height ratio for different water depths.

The crest to height ratio in Table 3 indicates asymmetric waves. The Airy theory assumes symmetrical waves. An expansion of the Airy theory with non-linear terms is therefore more likely to give better approximation of the wave kinematics. A widely used expansion of the Airy theory in engineering applications is Stokes 2nd order wave theory. This theory is almost as easy and fast to use as the Airy theory, and like the Airy theory, it is often used in first approximation of wave kinematics [6]. Stokes 2nd order theory will therefore be used to calculate the particle velocity.

The plot in Figure 5 indicates that the numerical stream function theory is applicable for the metocean data from the West Nile Delta. This theory will therefore be applied to calculate particle velocity near the seabed and the results will be compared with the approximations from the intermediate Airy theory described in DNV-RP-C205 and the 2nd order Stokes wave theory.

2.4 Stokes wave theory

Stokes wave theory is an analytical finite-amplitude theory. The wave parameters are expressed in terms of power series that truncated at a chosen order. Hence, Stokes 2nd order theory is truncated after the second term in the power series [6]. Unlike linear waves, the crest height A_C is larger than the trough height A_T. Hence, the waves are asymmetric.

2.4.1 Stokes 2nd order wave theory

Stokes 2nd order wave theory is widely used in engineering applications. The velocity potential is given by [6]

$$\Phi = \frac{gH}{2\omega}\frac{cosh\, k(d+z)}{cosh\, kd}sin(kx-\omega t) + \frac{3}{8}\frac{\pi H}{kT}\left(\frac{\pi H}{\lambda}\right)\frac{cosh\, 2k(d+z)}{sinh^4(kd)}sin(kx-\omega t) \qquad (20)$$

where g is the acceleration of gravity, H *is the* wave height, ω is the angular velocity, k is the wave number, d is the water depth, z is distance below the SWL, x spatial position along the x-axis, t is time, T is the wave period and λ is the wavelength.

Steeper crests and wider troughs are characteristic for 2nd order Stoke waves, and these waves have the following surface elevation η [6]

$$\eta = \frac{H}{2}cos(kx-\omega t) + \frac{\pi H^2}{8\lambda}\frac{cosh\, kd\,(2+cosh\, 2kd)}{sinh^3\, kd}cos\, 2(kx-\omega t) \qquad (21)$$

where H *is the* wave height, k is the wave number, x spatial position along the x-axis, ω is the angular velocity, t is time, λ is the wavelength, k is the wave number and d is the water depth.

The surface elevation profile in Stokes 2nd order theory given in equation (21), consists of two terms. The first term is equal to the expression of the surface elevation in Airy theory, equation (7). The second term in equation (21) represents the non-linear expansion. The surface elevation profile for both wave theories at a 50 meter water

depth is plotted in Figure 6. As expected, the 2nd order Stokes waves have steeper and higher crests than the symmetric waves in Airy theory [10].

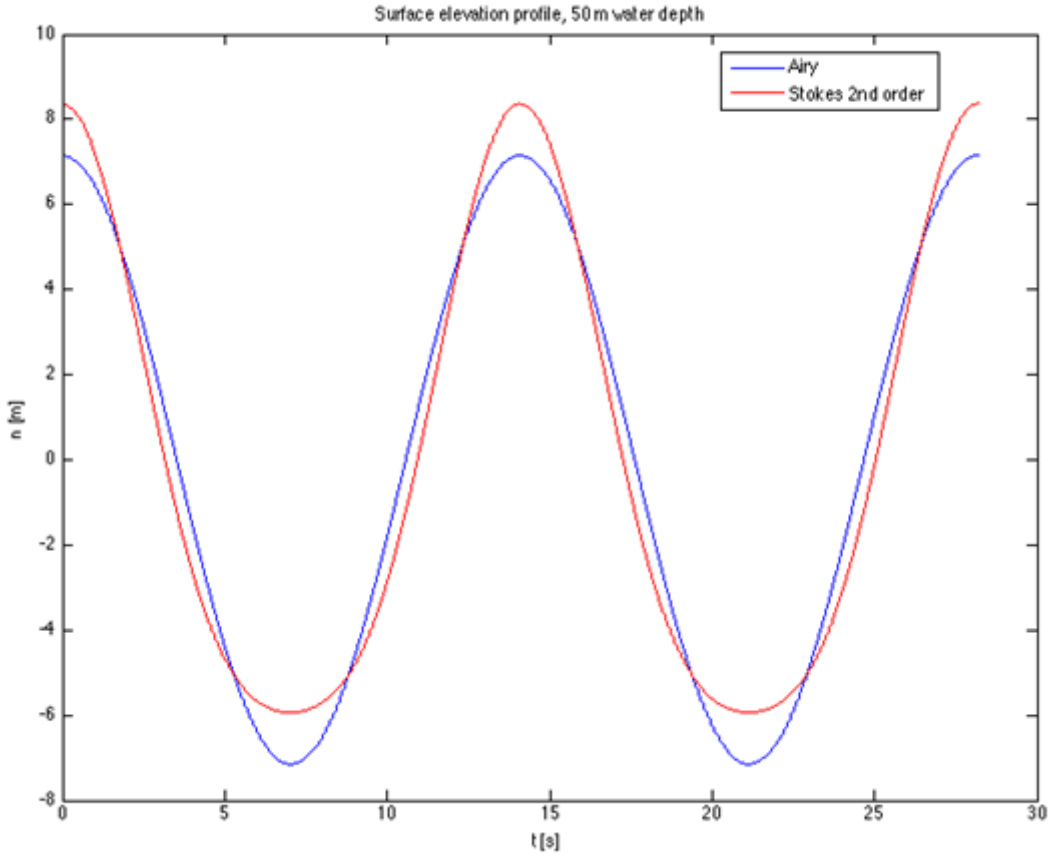

Figure 6: Surface elevation profile of waves at 50 meter water depth using Airy and 2nd order Stokes theory.

Stokes 2nd order theory holds on to the Airy theory's simplicity, because the linear dispersion relation is valid. Hence, the phase velocity c and wavelength λ are independent of the wave height, as for the linear Airy wave theory. This does not hold for 3rd or higher order Stokes wave theory [10].

In [6], Sorensen derived the following expressions for the horizontal and vertical particle velocity u and w using 2nd order Stokes wave theory

$$u = \frac{\pi H}{T}\frac{\cosh k(d+z)}{\sinh kd}\cos(kx-\omega t) + \frac{3(\pi H)^2}{4T\lambda}\frac{\cosh 2k(d+z)}{\sinh^4(kd)}\cos 2(kx-\omega t) \qquad (22)$$

$$w = \frac{\pi H}{T}\frac{sinh\, k(d+z)}{sinh\, kd} sin(kx - \omega t) + \frac{3(\pi H)^2}{4T\lambda}\frac{sinh\, 2k(d+z)}{sinh^4(kd)} sin\, 2(kx - \omega t) \qquad (23)$$

where *H is the* wave height, *T* is the wave period, *k* is the wave number, *d* is the water depth, *z* is the distance from the SWL, *x* spatial position along the x-axis, ω is the angular velocity, *t* is time and λ is the wavelength.

Notice that the first term in all Stokes 2nd order wave theory equations is equal to the expressions from the linear Airy theory.

2.5 Stream function theory

The stream function theory is a numerical procedure to obtain an exact solution to non-linear wave problems. The approach is to expand a stream function, represented by the water depth *d*, the wave height *H* and the wave period *T*, into numerically solvable Fourier series [14]. This method is, unlike the Airy theory method, time consuming and not straightforward in application. The theory was first presented by Dean in 1965 and the theory has been further developed to be valid for the highest possible waves by Rienecker and Fenton among others [15; 16]. In comparison with experimental values of particle velocity, the stream function theory have shown to provide significantly better results overall than other wave theories [14].

2.5.1 Assumptions and governing equations

As for the linear Airy theory, the flow in stream function theory is assumed to be ideal and in two dimensions. Ideal flow means that the fluid is incompressible and the flow is irrotational. The wave motion is also assumed to be periodic in x-direction. By subtracting the wave celerity, the wave motion is converted to steady flow in the x-direction. Thus, the stream function becomes constant at the free surface and on the horizontal seabed [6]. Hence, the governing equation is the Laplace equation represented in terms of the stream function $\psi(x, z)$ [15]

$$\frac{\partial^2 \psi}{\partial x^2} + \frac{\partial^2 \psi}{\partial z^2} = 0 \tag{24}$$

where *x* is the horizontal coordinate and *z* is the vertical coordinate referenced to the SWL and positive upwards.

The horizontal velocity component u_ψ and the vertical component w_ψ is defined as [15]

$$u_\psi = -\frac{\partial \psi}{\partial z} \tag{25}$$

$$w_\psi = \frac{\partial \psi}{\partial x} \tag{26}$$

where ψ is the stream function, z and x is respectively the vertical and horizontal coordinate referenced to the SWL.

2.5.2 Boundary conditions

In addition to the assumptions, boundary conditions are required to be imposed at the surface and at the seabed to formulate the numerical problem [14]

Bottom Boundary Condition (BBC)

The Bottom Boundary Condition (BBC) impose the following expressions for the vertical velocity component w and the vertical coordinate z at the seabed [14]

$$w_\psi = 0, \quad z = -d \tag{27}$$

where d is the water depth.

Kinematic Free Surface Boundary Condition (KFSBC)

The Kinematic Free Surface Boundary Conditions (KFSBC) applies to both the bottom and the surface and is given by [14]

$$\frac{\partial \eta_\psi}{\partial t} + u_\psi \frac{\partial \eta_\psi}{\partial x} = w_\psi, \quad z = \eta_\psi(x,t) \tag{28}$$

where η_ψ is the surface elevation, t is time, u_ψ is the horizontal velocity component, x is the horizontal coordinate, w_ψ is the vertical velocity component and z is the vertical coordinate referenced to the SWL and positive upwards.

Dynamic Free Surface Boundary Condition (DFSBC)

The Dynamic Free Surface Boundary Condition (DFSBC) imposes that the pressure below the free surface is uniform and equal to the atmospheric pressure P_a [14]

$$\eta_\psi + \frac{P_a}{\rho g} + \frac{u_\psi^2 + w_\psi^2}{2g} - \frac{1}{g}\frac{\partial \Phi_\psi}{\partial t} = constant = Q, \quad z = \eta_\psi(x,t) \tag{29}$$

where η_ψ is the surface elevation, ρ is the density, g is the acceleration of gravity, u_ψ is the horizontal velocity component, w_ψ is the vertical velocity component, Φ_ψ is the velocity potential, t is time, x is the horizontal coordinate and Q is Bernoulli's constant for steady flow.

2.5.3 The stream function solution

Dean expresses in [14] that the solution to the stream function ψ is obtained by using equation (24) and imposing the boundary conditions given in equation (27), (28) and (29)

$$\psi(x,z) = \frac{\lambda_\psi}{T} z + \sum_{n=1}^{N} X(n)\, sinh\left(\frac{2\pi n}{\lambda_\psi}(d+z)\right) cos\left(\frac{2\pi n}{\lambda_\psi} x\right) \tag{30}$$

where z is the vertical coordinate referenced to the SWL and positive upwards, λ_ψ is the wavelength, T is the wave period, N is the chosen order of the wave theory, $X(n)$ represents the stream function coefficients, n is index, d is the water depth and x is the horizontal coordinate.

Equation (30) satisfy the Laplace equation (24), the BBC (27) and the KFSBC (28) for arbitrary values of the so far undetermined values of the wavelength λ_ψ and the stream function coefficients $X(n)$. The last boundary condition, the DFSBC (29) is satisfied by numerical iteration of the values of the wavelength λ_ψ and the stream function coefficients $X(n)$ [14]. Dean has in [17] tabulated 40 cases for different wave conditions. The tabulated values assume zero water current. Applicable cases are dependent on relative depth and wave steepness, as shown in Figure 7.

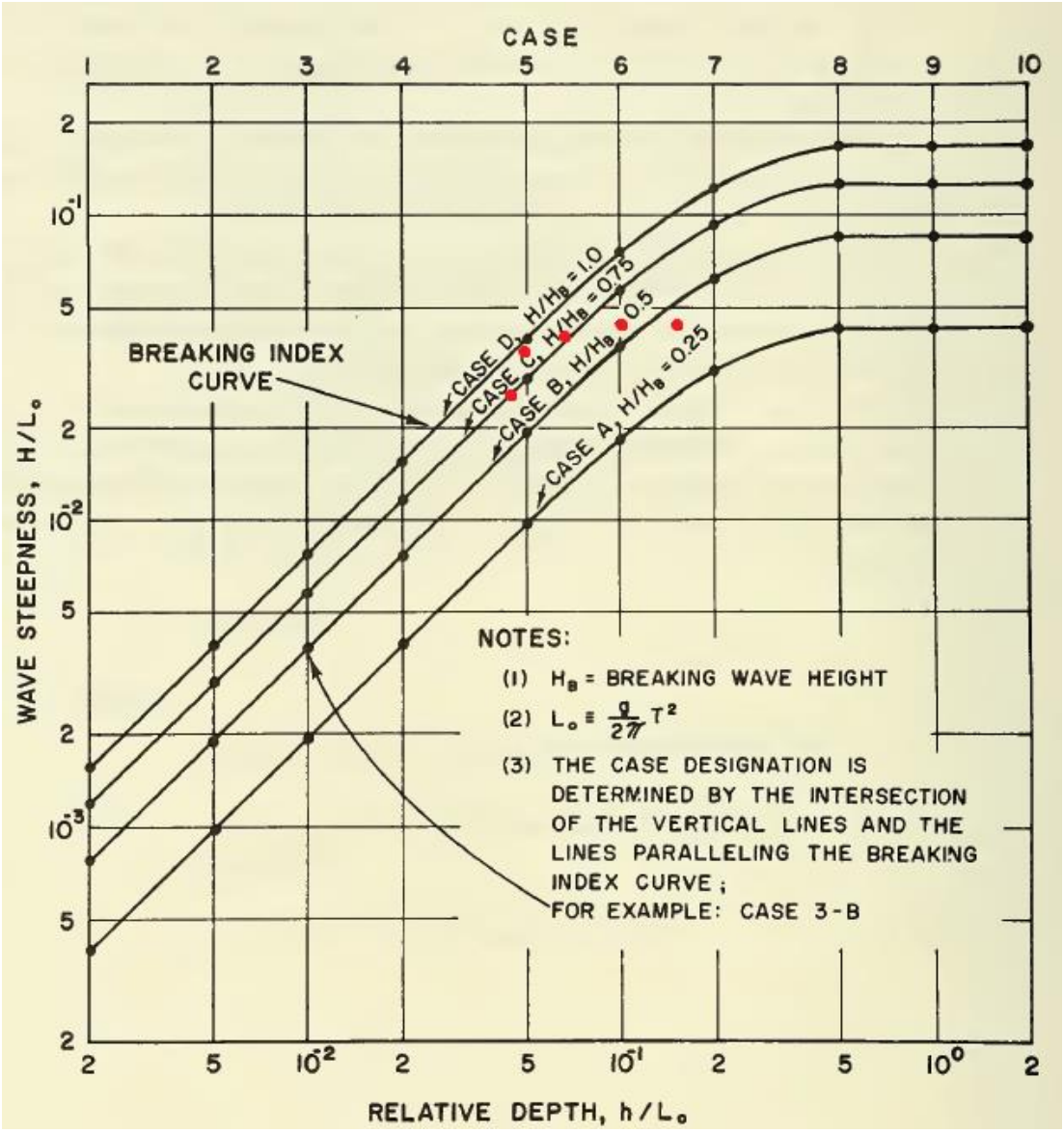

Figure 7: Applicable cases to extract stream function coefficients and wavelengths [17].

The red points in Figure 7 represent the wave data from the West Nile Delta. The points do not fit perfectly with the given cases. Therefore, the values of the stream function coefficients *X(n)* and the wavelengths λ_ψ are extracted from [17] by interpolation between the different cases for the water depth range. Applied cases in the interpolation for each water depth are listed in Table 4.

Water depth [m]	Case
10	4-C, 5-C
15	5-C, 5-D
25	5-C, 6-C
35	6-B, 6-C
50	6-A, 6-B, 7-A, 7-B

Table 4: Cases applied when extracting stream function coefficients and wavelengths.

The stream function coefficients and wavelengths are extracted by interpolation of the table values in [17] and listed in Table 5 and Table 6.

Water depth [m] / Stream function coefficients	10	15	25	35	50
X(1)	43.2573	62.6982	101.6416	97.5062	74.1016
X(2)	8.7466	14.4643	15.3981	9.7630	1.1413
X(3)	1.7156	3.5238	2.4441	0.8023	0.0025
X(4)	0.3007	0.7861	0.3819	0.0508	1.3080E-04
X(5)	0.0461	0.1802	0.0559	0.0025	5.7393E-06
X(6)	0.0060	0.0376	0.0145	2.1767E-04	*
X(7)	6.5552E-04	0.0095	8.2613E-04	9.8497E-05	*
X(8)	8.9287E-05	0.0020	1.0558E-04	*	*
X(9)	5.4214E-05	8.6511E-04	6.4106E-05	*	*
X(10)	*	6.7755E-04	*	*	*

Table 5: Values of applicable stream function coefficients for different water depths.
*** Stream function is of lower order.**

Water depth [m]	Wavelength λ_ψ [m]	Wavelength λ (Airy)
10	140.6731	120.6200
15	187.3456	161.1862
25	229.6835	210.6406
35	233.6366	228.1658
50	265.7766	259.7194

Table 6: Tabulated stream function wavelength λ_ψ and approximated wavelength λ in Airy theory.

Surface elevation

By rearranging equation (30) and setting $z = \eta_\psi$, the expression for the surface elevation η_ψ at the free surface is [14]

$$\eta_\psi = \frac{T}{\lambda_\psi}\psi_{\eta_\psi} - \frac{T}{\lambda_\psi}\sum_{n=1}^{N}\left[X(n)sinh\left(\frac{2\pi n}{\lambda_\psi}(d+\eta_\psi)\right)cos\left(-\frac{2\pi n}{T}t\right)\right] \tag{31}$$

where T is the wave period, λ_ψ is the wavelength, ψ_{η_ψ} is the solution of the stream function with $z = \eta_\psi$, N is the order of the wave theory, $X(n)$ represents the stream function coefficients, n is index, d is the water depth and x is the horizontal coordinate.

Particle velocity

In [14], Dean computes the following expressions for the horizontal u_ψ and vertical particle w_ψ

$$u_\psi = -\sum_{n=1}^{N}\left[X(n)\left(\frac{2\pi}{\lambda_\psi}n\right)cosh\left(\frac{2\pi}{\lambda_\psi}nS\right)cos\big(n(kx-\omega t)\big)\right] \tag{32}$$

$$w_\psi = -\sum_{n=1}^{N}\left[X(n)\left(\frac{2\pi}{\lambda_\psi}n\right)sinh\left(\frac{2\pi}{\lambda_\psi}nS\right)sin\big(n(kx-\omega t)\big)\right] \tag{33}$$

where $X(n)$ represents the stream function coefficients listed in Table 5, λ_ψ is the wavelength, n is index, S is the vertical coordinate referenced to the bottom and positive upwards, k is the wave number, x is the horizontal coordinate, ω is the angular frequency and t is time.

3. Boundary layer theory

The wave theories that have so far been included in this thesis neglects boundary layer effects on the wave flow close to the seabed. In this chapter, a literature research in boundary layer theory will be carried out. Stokes oscillating boundary layer theory will be described in detail and used to evaluate boundary layer effects on the wave flow. A brief introduction to turbulent boundary layer theory is also included in this chapter. Basic principles of sediment transport near the seabed will be included in the last section.

3.1 Introduction

The waves from the West Nile Delta are non-breaking waves propagating over a silty sand seabed. Shear stress caused by the roughness of the seabed and possible sediment transport of sand in the water affects the wave flow. Figure 8 illustrates how the boundary layer, with thickness δ, affects the velocity profile near the seabed. In the boundary layer region, potential theories as the Airy theory, 2nd order Stokes wave theory and the stream function theory are not valid, because shear stress becomes important. The Navier-Stokes equation with boundary layer approximations is applicable for the flow in the boundary layer [18].

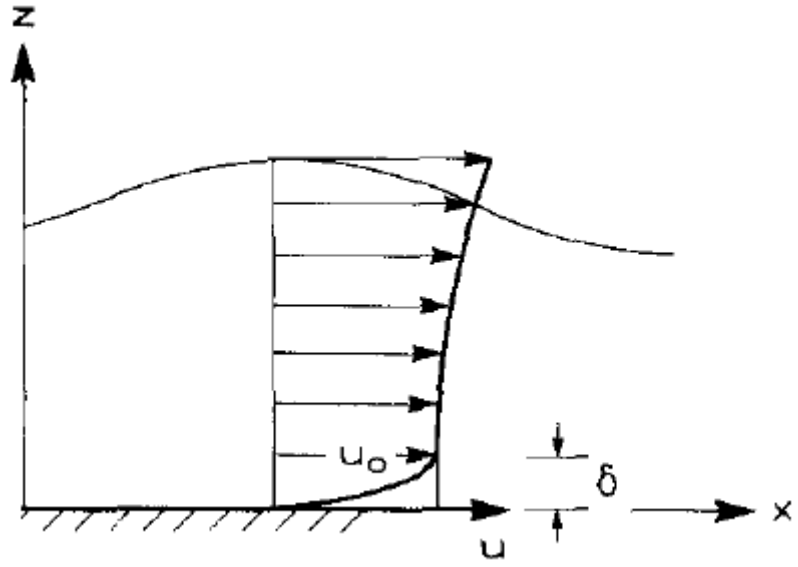

Figure 8: Velocity profile with boundary layer close to the seabed [18].

3.2 Boundary layer modelling

In this thesis, the boundary layer is assumed to be pure oscillatory. An oscillatory boundary layer is caused by a uniform oscillating flow [18], which is applicable for the waves from the West Nile Delta. The wave flow is evaluated by examine the horizontal flow velocity u. An expression for the horizontal velocity u can be derived using Stokes oscillating boundary layer theory, or by examining the governing equations for the boundary layer flow directly.

3.2.1 Stokes oscillating boundary layer

Stokes oscillating boundary layer is a boundary layer caused by an oscillating flow of a viscous fluid over a solid wall. The boundary layer is named after the Irish mathematician and physicist, Sir George Gabriel Stokes. He was the first to derive an analytical solution to the Navier-Stokes equation for a boundary layer caused by laminar flow over a smooth wall [19; 20]. For turbulent flow, a numerical approach is necessary to obtain a solution to the Navier-Stokes equation.

Governing equations

The oscillating flow is assumed to be unidirectional and parallel to the seabed. As for the other theories described in this thesis, the fluid is assumed to be incompressible. This assumption is valid where the fluid velocity is small compared to the speed of sound in the respectively fluid. The fluid density is assumed to not vary significantly. With these assumptions, the Navier-Stokes equation is given as [19]

$$\frac{\partial u}{\partial t} + u\frac{\partial u}{\partial x} = -\frac{1}{\rho}\frac{\partial p}{\partial x} + \nu\frac{\partial^2 u}{\partial z^2} \tag{34}$$

where u is the horizontal velocity, t is time, ρ is density, p is pressure, x is the horizontal coordinate, ν is the kinematic viscosity and z is the vertical coordinate referenced to the seabed.

Oscillation of a moving boundary

If a solid boundary moves with harmonic oscillations, viscous stresses are applied to the fluid close to the moving boundary. The velocity of the moving boundary is used as an boundary condition and given by the following expression [19]

$$u_{mb}(0,t) = U\,cos\,\omega t \tag{35}$$

where u_{mb} is the horizontal velocity to the moving boundary, U is the velocity amplitude, ω is the angular frequency and t is time.

Before the boundary is set in motion, the fluid is assumed to be at rest close to the boundary. The viscous stress from the boundary gives the fluid the following velocity distribution [19]

$$\frac{\partial u}{\partial t} = \nu \frac{\partial^2 u}{\partial z^2} \tag{36}$$

where u is the horizontal fluid velocity, t is time, ν is the kinematic viscosity and z is the vertical coordinate referenced to the moving boundary.

Equation (36) is the diffusion equation, widely used in thermodynamics. A second boundary condition is necessary to impose to obtain a solution to equation (36). This boundary condition concerns the horizontal fluid velocity u infinite from the moving boundary [19]

$$u \to 0, \quad z \to \infty \tag{37}$$

where z is the vertical coordinate referenced to the moving boundary.

The fluid velocity u gradually becomes a harmonic function of time, oscillating with the same frequency as the moving boundary. A complex exponential function is therefore used to derive an expression for the horizontal fluid velocity u [19]

$$u(z,t) = Re\{e^{i\omega t}F(z)\} \tag{38}$$

where *Re* denotes the real part of the complex expression, ω is the angular frequency, t is time and F is a function depending on the vertical coordinate z referenced to the moving boundary.

The expression for the fluid velocity u from equation (38) is combined with equation (36) and the following expression is obtained [19]

$$i\ \omega\ F = \nu \frac{\partial^2 F}{\partial z^2} \tag{39}$$

where ω is the angular frequency, F is a function depending on the vertical coordinate z referenced to the moving boundary and ν is the kinematic viscosity.

The only solution that satisfies the boundary condition stated in equation (37) is [19]

$$F(z) = A\ e^{-(1+i)(\frac{\omega}{2\nu})^{1/2}\ z} \tag{40}$$

where F is a function depending on the vertical coordinate z referenced to the moving boundary, A is the integrating constant, ω is the angular frequency and ν is the kinematic viscosity.

The first boundary condition, equation (35), states that the velocity of the fluid is equal to the velocity of the moving boundary at $z = 0$. This implies that the integrating constant A must be equal to the velocity amplitude U. The solution of the horizontal fluid velocity u is now obtained [19]

$$u(z,t) = U\ e^{-\left(\frac{\omega}{2\nu}\right)^{1/2} z}\ cos\left[\omega t - \left(\frac{\omega}{2\nu}\right)^{1/2}\ z\right] \tag{41}$$

where U is the velocity amplitude, ω is the angular frequency, ν is the kinematic viscosity, z is the vertical coordinate referenced to the moving boundary and t is time.

3.2.2 Boundary layer flow

In [18], Fredsoe and Deigaard use a different approach to derive a solution to the horizontal particle velocity in the boundary layer, applying the boundary layer flow equation directly. The boundary layer flow equation is given as

$$\rho \frac{du}{dt} = \rho \left(\frac{\partial u}{\partial t} + u \frac{\partial u}{\partial x} + w \frac{\partial u}{\partial z} \right) = -\frac{\partial p}{\partial x} + \frac{\partial \tau}{\partial z} \tag{42}$$

where ρ is the density, u is the horizontal velocity, t is time, x is the horizontal coordinate, w is the vertical velocity, z is the vertical coordinate referenced to the seabed, p is the pressure and τ is the shear stress.

The pressure p is zero in the z-direction, because it is perpendicular to the flow direction. The assumption of uniform flow reduce equation (42) to [18]

$$\rho \frac{\partial u}{\partial t} = -\frac{\partial p}{\partial x} + \frac{\partial \tau}{\partial z} \tag{43}$$

where ρ is the density, u is the horizontal velocity, t is time, x is the horizontal coordinate, z is the vertical coordinate referenced to the seabed, p is the pressure and τ is the shear stress.

Outside the boundary layer, the shear stress τ is zero. Hence, equation (43) is reduced to the following expression outside the boundary layer [18]

$$\rho \frac{\partial u_o}{\partial t} = -\frac{\partial p}{\partial x} \tag{44}$$

where ρ is the density, u_o is the free stream velocity, t is time, x is the horizontal coordinate and p is the pressure.

The equation for the flow inside the boundary layer is obtained by combining equation (43) and (44)

$$\rho \frac{\partial}{\partial t}(u_0 - u) = -\frac{\partial \tau}{\partial z} \tag{45}$$

where ρ is the density, t is time, u_o is the free stream velocity, u is the horizontal velocity, z is the vertical coordinate referenced to the seabed and τ is the shear stress.

The wave boundary layer thickness δ, also called Stokes length, is an important parameter in boundary layer theory and is expressed as

$$\delta = \sqrt{\frac{2\nu}{\omega}} \tag{46}$$

where ν is the kinematic viscosity and ω is the angular frequency.

Laminar boundary layer

In the case of uniform flow, fluid flows without significant mixing among the layers and the flow is laminar [21]. In the laminar boundary layer, the shear stress τ is given as [18]

$$\frac{\tau}{\rho} = \nu \frac{\partial u}{\partial z} \tag{47}$$

where ρ is the density, ν is the kinematic viscosity, u is the horizontal velocity, z is the vertical coordinate referenced to the seabed and τ is the shear stress.

By using the relation from equation (47) in equation (45), the follow expression is obtained [18]

$$\rho \frac{\partial}{\partial t}(u_0 - u) = -\nu \frac{\partial^2 u}{\partial z^2} \tag{48}$$

with

$$u_o = U\, sin(\omega t) \tag{49}$$

where ρ is the density, t is time, u_o is the free stream velocity, u is the horizontal velocity, ν is the kinematic viscosity, z is the vertical coordinate referenced to the seabed, U is the amplitude of the near-bed velocity and ω is the angular frequency.

To solve equation (48) for the horizontal velocity u, two boundary conditions concerning the horizontal fluid velocity at the seabed and infinite far from the seabed are imposed [18]

$$u = 0, \quad z = 0 \tag{50}$$

$$u \to u_0, \quad z \to \infty \tag{51}$$

where z is the vertical coordinate referenced to the seabed and u_o is the free stream velocity.

Horizontal fluid velocity

In [18], the solution of equation (48) is obtained by using the relation in equation (49) and the boundary conditions given in (50) and (51)

$$u = U\,sin(\omega t) - Ue^{\left(-\frac{z}{\delta}\right)} sin(\omega t - \frac{z}{\delta}) \tag{52}$$

where u is the horizontal fluid velocity, U is the amplitude of the near-bed velocity, ω is the angular frequency, t is time, z is the vertical coordinate referenced to the seabed and δ is the boundary layer thickness.

The expression in equation (52) is consistent with the expression derived for an oscillating flow using Stokes oscillating boundary layer. This will now be shown. In the case of an oscillating flow, the Navier-Stokes equation is given in equation (34). The variation in x-direction is neglected within the boundary layer. Hence, the non-linear term $u\frac{\partial u}{\partial x}$ is removed from the Navier-Stokes equation.

The pressure gradient in equation (34) is represented with the function $G(t)$. This term cannot be neglected for an oscillating flow of a fluid, because pressure gradient needs to be present to change the flow direction. With these two assumptions, the Navier-Stokes equation is now written as

$$\frac{\partial u}{\partial t} = -\frac{1}{\rho} G(t) + \nu \frac{\partial^2 u}{\partial z^2} \tag{53}$$

where u is the horizontal fluid velocity, t is time, ρ is density, ν is the kinematic viscosity and z is the vertical coordinate referenced to the seabed.

Boundary conditions concerning the horizontal velocity u at the seabed and infinite away from the seabed are imposed

$$u(0, t) = 0 \tag{54}$$

$$u(\infty, t) = U\, cos(\omega t - \beta) \tag{55}$$

where U is the velocity amplitude, ω is the angular frequency, t is time and β is a phase angle.

The horizontal fluid velocity u can now be expressed as

$$u(z, t) = U\, cos(\omega t - \beta) - u_{mb}(z, t) \tag{56}$$

where U is the velocity amplitude, ω is the angular frequency, t is time, β is a phase angle and u_{mb} is the velocity of the moving boundary.

The relation in equation (56) combined with equation (53) gives

$$\frac{\partial}{\partial t}(U\, cos(\omega t - \beta)) = -\frac{1}{\rho} G(t) \tag{57}$$

where U is the velocity amplitude, ω is the angular frequency, t is time, β is a phase angle, ρ is density and $G(t)$ is a function that represents the pressure gradient.

The Navier-Stokes equation for the horizontal velocity in terms of the velocity to the moving boundary u_{mb} is

$$\frac{\partial u}{\partial t} = \nu \frac{\partial^2 u_{mb}}{\partial z^2} \tag{58}$$

with boundary conditions

$$u_{mb}(0,t) = U\,cos(\omega t - \beta) \tag{59}$$

$$u(\infty,t) = 0 \tag{60}$$

where u is the horizontal fluid velocity, t is time, ν is the kinematic viscosity, z is the vertical coordinate referenced to the seabed, U is the velocity amplitude, ω is the angular frequency and β is a phase angle.

The solution of the horizontal velocity u is obtained by using the relations in equation (56) and (58) with the expression obtained in (41)

$$u(z,t) = U\,cos(\omega t - \beta) - U\,e^{-\left(\frac{\omega}{2\nu}\right)^{1/2} z} cos\left[\left(\frac{\omega}{2\nu}\right)^{1/2} z - \omega t + \beta\right] \tag{61}$$

where U is the velocity amplitude, ω is the angular frequency, t is time, β is a phase angle, ν is the kinematic viscosity and z is the vertical coordinate referenced to the seabed.

The horizontal velocity is expressed as a sine function by Fredsoe and Deigaard in [18]. Hence, trigonometric identities are used to phase shift the expression in (61) from cosine to sine to show consistency between the two expressions. The relationship between cosine and sine is

$$\cos(\omega t - \beta) = \sin(\omega t)\,, \quad \beta = \frac{\pi}{2} \tag{62}$$

where ω is the angular frequency, t is time, β is a phase angle.

By setting the phase angle $\beta = \frac{\pi}{2}$ and using the boundary layer thickness expressed in equation (46) in equation (61), the following expression for the horizontal fluid velocity u is obtained

$$u(z,t) = U\sin(\omega t) - U\,e^{-\frac{z}{\delta}}\sin\left[\omega t - \frac{z}{\delta}\right] \tag{63}$$

where U is the velocity amplitude, ω is the angular frequency, t is time, z is the vertical coordinate referenced to the seabed and δ is the boundary layer thickness.

Equation (63) is equal to the expression derived by Fredsoe and Deigaard in [18] given in equation (52).

3.2.3 Turbulent boundary layer

Turbulence is a flow regime where the flow velocity and pressure vary rapid and almost randomly in space and time. Turbulent flow contains small eddies with different velocity gradients. Hence, fluctuations occur and there is continuous mixing of particles in turbulent flow [22]. Figure 9 illustrates the conceptual differences between the laminar and turbulent boundary layer. Due to the chaotic nature of turbulence, complex and expensive numerical tools have to be used to predict turbulent fluid motion.

Figure 9: Illustration of laminar and turbulent boundary layer.

The momentum integral method

The momentum integral method is a flow model that can be used in the turbulent boundary layer. Equation (45) is applicable for both laminar and turbulent flow. The momentum integral method is a method where the wave boundary layer is modelled by a momentum equation. The method has shown to give an accurate approximation to the bed shear stress τ_b. The following momentum equation is derived by integrating equation (45) over the boundary layer thickness δ with the assumption that the shear stress is zero at the top of the boundary layer [18]

$$-\rho \int_{z_o}^{\delta+z_o} \frac{\partial}{\partial t}(u_o - u)dz = \int_{z_o}^{\delta+z_o} \frac{\partial \tau}{\partial z} dz = -\tau_b \qquad (64)$$

where ρ is the density, z_o is the bottom roughness parameter, t is time, u_o is the free stream velocity, u is the horizontal velocity, z is the vertical coordinate referenced to the seabed, τ is the shear stress and τ_b is the bed shear stress.

The bed shear stress $\tau_b$is calculated by using equation (64). This is a key parameter in wave boundary and sediment transport modelling. More sophisticated numerical models have been developed to calculate the bed shear stress, but all models give the same results with very little deviations [18].

Velocity profile approximation

To solve the momentum equation in (64), the shape of the velocity profile must fit the given boundary conditions in (50) and (51). The West Nile Delta's silty sand seabed is characterized as hydraulically rough. A hydraulically rough seabed has the following logarithmic approximation for the horizontal velocity profile [18]

$$u = \frac{U_f}{\kappa} ln\left(\frac{z}{z_o}\right) \qquad (65)$$

with

$$U_f = \sqrt{\frac{|\tau_b|}{\rho}} \qquad (66)$$

where u is the horizontal velocity, U_f is the friction velocity, κ is von Kármán's constant, z is the vertical coordinate referenced to the seabed, z_o is the bed roughness parameter, τ_b is the bed shear stress and ρ is the density.

The approximation of logarithmic velocity profile has shown to give small deviations with results from complex numerical models close to the seabed [18].

3.3 Viscosity

Viscosity, or dynamic viscosity μ, is defined as the shear stress to velocity gradient ratio. A simpler and more physical description of viscosity is that it is a measure of a fluid resistant to flow. The dynamic viscosity μ is depending on fluid properties and varies with temperature. In fluid dynamics, the viscosity often refers to the kinematic viscosity ν. The kinematic viscosity ν is given as [19]

$$\nu = \frac{\mu}{\rho} \tag{67}$$

where μ is the dynamic viscosity and ρ is the density of the fluid.

3.3.1 Eddy viscosity

The eddy viscosity ν_T describes the turbulence and varies vertically in the boundary layer. With a model for the eddy viscosity ν_T in the boundary layer, an exact solution to the flow equation given in equation (45) can be obtained. Eddy viscosity ν_T is expressed as [18]

$$\frac{\tau}{\rho} = \nu_T \frac{\partial u}{\partial z} \tag{68}$$

where τ is the shear stress, ρ is the density, u is the horizontal velocity and z is the vertical coordinate referenced to the seabed.

Notice that, apart from the viscosity term, equation (68) is equal to equation (47) that describes the kinematic viscosity ν. In the case of a linear increasing eddy viscosity with the vertical coordinate z referenced to the seabed, Fredsoe and Deigaard derive the following expression for the eddy viscosity ν_T [18]

$$\nu_T = \kappa U_{f,max} z \tag{69}$$

where κ is von Kármán's constant , $U_{f,max}$ is the maximum friction velocity and z is the vertical coordinate referenced to the seabed.

By combining the linear approximation from equation (69) and the flow equation in equation (45), the boundary layer flow is [18]

$$\frac{\partial}{\partial t}(u - u_0) = -\frac{\partial}{\partial z}\left(\kappa U_f z \frac{\partial(u-u_0)}{\partial z}\right) \tag{70}$$

where t is time, u is the horizontal velocity, u_o is the free stream velocity, z is the vertical coordinate referenced to the seabed, κ is von Kármán's constant and U_f is the friction velocity.

Equation (70) can be solved analytically. The calculated velocity profile has a logarithmic shape. Several other and more complex eddy viscosity models have been developed, with small deviations in approximated velocity profile [18].

3.3.2 Stokes oscillating boundary layer with variable viscosity

A dimensionless solution to Stokes oscillating boundary layer with variable viscosity is now derived. The eddy viscosity ν_T is assumed to be dependent on the vertical coordinated z referenced to the moving boundary. Equation (36) with variable viscosity is

$$\frac{\partial u}{\partial t} = \frac{\partial}{\partial z}\left(\nu_T(z)\frac{\partial u}{\partial z}\right) \tag{71}$$

where u is the horizontal velocity, t is time, $\nu_T(z)$ is the eddy viscosity depending on the vertical coordinate z referenced to the moving boundary.

At the moving boundary, the velocity is given in equation (35). As for Stokes oscillating boundary layer with constant viscosity, the flow becomes a harmonic function of time and will oscillate with the same frequency as the moving boundary. The fluid velocity is therefore given by the following complex expression

$$u(z,t) = Re\{U\, Z(z) e^{i\omega t}\} \tag{72}$$

where U is the velocity amplitude, Z is a function dependent on the vertical coordinate z referenced to the moving boundary, ω is the angular frequency and t is time.
Equation (72) inserted in equation (71) gives the following expression

$$i\,\omega\,Z = \frac{\partial}{\partial z}\left(\nu_T(z)\frac{\partial Z}{\partial z}\right) \tag{73}$$

where ω is the angular frequency, Z is a function and $\nu_T(z)$ is the eddy viscosity, both dependent on the vertical coordinate z referenced to the moving boundary.

The following boundary conditions is imposed to equation (73)

$$Z(0) = 1 \tag{74}$$

$$Z(\infty) = 0 \tag{75}$$

where Z is a function depending on the vertical coordinate z referenced to the seabed.

To solve equation (73), the eddy viscosity ν_T dependency on the vertical coordinate z must be approximated. This approximation is done by using power series and is described in the following section.

3.3.3 Power series

Power series is an important part in function analysis. A power series is an infinite series on the form

$$f(x) = \sum_{n=0}^{\infty} a_n(x-c)^n \tag{76}$$

where $f(x)$ is a function depending on x, n is the index, a_n is the coefficients of nth order and c is a constant.

Taylor series is an expansion of a function about a single point. The Taylor series of a function $f(x)$ is expanded to an infinite series of the functions derivatives about the point $x = a$ and given as [23]

$$f(x) = \sum_{n=0}^{\infty} \frac{f^n(a)}{n!}(x-a)^n \tag{77}$$

where n is the order of the Taylor series.

For the special case of $a = 0$, the power series is called a Maclaurin series. A Taylor series have infinite amount of singularities. A singularity is a point where the function's value is not defined. Truncated Taylor series is a type of Taylor series that is limited to a specific index *n*. The variable viscosity is evaluated from zero to infinity. In that case, both Taylor series and truncated Taylor series go to infinity and do not approximate a defined value of the viscosity. This is a problem in the viscosity approximation, since the viscosity does not go to infinity when the dimensionless distance *Z* from the moving boundary increases. The power series should converge to a defined value in the approximation of the viscosity. Therefore, Taylor series is not applicable to approximate the variable viscosity in this case.

Padé approximant

Padé approximant is a type of rational approximation that in most cases are superior to Taylor series for complex functions with singularities. This is because rational functions only have singularities in the extended complex plane. Another advantage with Padé approximant is that the error is distributed over a bigger interval than for truncated Taylor series. The Padé approximation $P(x)$ is an expansion of a function as a ratio of two power series and can be expressed as [24]

$$P(x) = \frac{\sum_{i=0}^{m} a_i x^i}{1+\sum_{j=0}^{n} b_j x^j} \tag{78}$$

where *m, n* is the order of the rational function and a_i, b_j are arbitrary coefficients.

In the calculations in this thesis, the approximation of the dimensionless eddy viscosity ν_T is restricted to the following 1st order Padé approximant

$$\nu_T(z) = \frac{1+Az}{1+z} \tag{79}$$

where $\nu_T(z)$ is the dimensionless eddy viscosity, A is an arbitrary coefficient and z is the dimensionless vertical coordinate referenced to the boundary.

A weakness with the 1st order Padé approximation is that the viscosity gradient is determined by the coefficient A. This can be avoided by using 2nd or higher order Padé approximant.

The 1st order Padé approximant is used to approximate the variable viscosity. The approximated variable viscosity is inserted in equation (73) to obtain a numerical solution to evaluate the horizontal velocity distribution in the boundary layer.

3.3.4 Dimensionless description of Stokes boundary layer

The relationship between the dimensionless displacement and dimensionless velocity will now be evaluated. The velocity expression in equation (41) in Stokes oscillating boundary layer theory can be transformed to a dimensionless expression by inserting following dimensionless parameters

$$z' = \frac{z}{\delta}, \quad t' = \omega t, \quad u' = \frac{u}{U} \tag{80}$$

where z is the vertical coordinate, δ is the boundary layer thickness, ω is the angular frequency, t is time, u is the horizontal velocity and U is the velocity amplitude.

Equation (41) is now transformed to the following dimensionless expression

$$u'(z', t') = e^{-z'}\cos(z' - t') \tag{81}$$

where $u'$is the dimensionless horizontal velocity, z' is the dimensionless vertical coordinate and t' is the dimensionless time.

The apostrophes are dropped in the further description. The relation between the dimensionless horizontal velocity u and the displacement function $X(z,t)$ is given as

$$u(z,t) = e^{-z}\cos(z-t) = \dot{X}(z,t) \tag{82}$$

where z is the dimensionless vertical coordinate and t is the dimensionless time.

Integrating equation (82) gives the displacement function $X(z,t)$

$$X(z,t) = e^{-z}\sin(z-t) \tag{83}$$

where z is the dimensionless vertical coordinate and t is the dimensionless time.

Equation (83) describes the displacement function $X(z,t)$. The relationship between this function and the dimensionless horizontal velocity is represented in the phase diagram in Figure 12. The graphs plotted vary with dimensionless distance *Z,* but the *Z*-value is not explicit defined. Nevertheless, the phase diagram is able to gives an impression of the whole process in a two dimensional plot. The phase diagram also illustrates the relationship between the real and imaginary part of the solution to Stokes boundary layer with variable viscosity, given in equation (73).

3.4 Stream function theory with boundary layer effects

The horizontal particle velocity expression derived in the stream function theory is given in equation (32). This expression can be modified with Stokes oscillating boundary layer theory. Equation (32) at the seabed is

$$u_\psi|_{S=0} = -\sum_{n=1}^{N}\left[X(n)\left(\frac{2\pi}{\lambda_\psi}n\right)cos\big(n(kx-\omega t)\big)\right] \tag{84}$$

where S is the vertical coordinate referenced to the seabed, *X(n)* is the stream function coefficients, λ_ψ is the wavelength, *n* is index, *k* is the wave number, *x* is the horizontal coordinate, ω is the angular frequency and *t* is time.

Equation (84) is rewritten using trigonometric identities

$$u_\psi|_{S=0} = -\sum_{n=1}^{N}\left[X(n)\left(\frac{2\pi}{\lambda_\psi}n\right)(\cos(nkx)\cos(n\omega t)+\sin(nkx)\sin(n\omega t))\right] \tag{85}$$

where S is the vertical coordinate referenced to the seabed, *X(n)* is the stream function coefficients, λ_ψ is the wavelength, *n* is index, *k* is the wave number, *x* is the horizontal coordinate, ω is the angular frequency and *t* is time.

The expression from the Stokes oscillating boundary layer in equation (63) is inserted in equation (85) and the following expression for the horizontal velocity $u_\psi|_z$ is obtained

$$\begin{aligned} u_\psi|_z = -\sum_{n=1}^{N}\Bigg[&X(n)\left(\frac{2\pi}{\lambda_\psi}n\right)\cos(nkx)\left[\cos(n\omega t)-e^{-\frac{z}{\delta_n}}\cos(n\omega t-\frac{z}{\delta_n}\right] \\ &+X(n)\left(\frac{2\pi}{\lambda_\psi}n\right)\sin(nkx)\left[\sin(n\omega t)-e^{-\frac{z}{\delta_n}}\sin(n\omega t-\frac{z}{\delta_n}\right]\Bigg] \end{aligned} \tag{86}$$

with

$$\delta_n = \sqrt{\frac{2\nu}{n\omega}} \tag{87}$$

where z is the vertical coordinate referenced to the seabed, *X(n)* is the stream function coefficients, λ_{ψ} is the wavelength, *n* is index, *k* is the wave number, *x* is the horizontal coordinate, ω is the angular frequency, *t* is time, δ_n is the boundary layer thickness and ν is the kinematic viscosity.

The expression obtained in equation (86) is the horizontal velocity expression derived in stream function theory modified with Stokes boundary layer theory.

3.5 Sediment transport theory

Sediment transport is an important topic in coastal engineering, especially in the case of erosion on submerged structures [18]. Sediment transport may occur in the boundary layer near the seabed and it is a complex process, concerning turbulent flow of a dilute solution of suspended particles and seawater. Also, interaction between sediments and interaction between sediments and seawater contributes to high complexity of the dynamics near the seabed [25]. Several advanced numerical sediment transport models have been developed, but due to high sensitivity to variations in input data, the models developed have shown limited range of validity [18].

3.5.1 Sediment transport

Sediment transport mechanism above seabed is commonly divided in wash load, suspended load and bed load. Wash load includes very small particles that are not connected to the seabed and is therefore neglected in sediment transport models. There is no absolute limit between bed load and suspended load. The bed load consists of the sediments that are in continuous contact with the seabed, while suspended load refers to suspended sediments that are not in continuous contact with the seabed [18].

Bed roughness and sediment properties

The bed roughness is a key parameter to determine the bed load sediment transport. For a sandy seabed, like at the West Nile Delta, the bed roughness is dependent on the grain size of the sand. The bed roughness parameter z_0 is derived using Nikuradse's formulation [25; 26]

$$z_0 = \frac{2.5 d_{50}}{30} \tag{88}$$

where d_{50} is the median grain size of the silty sand.

The bottom bed roughness z_0 and the median grain size d_{50} for the West Nile Delta case are given in Table 2.

Settling velocity

In coastal engineering, the settling velocity refers to the terminal velocity when a grain is settling in a fluid. At this point, the frictional and buoyancy forces are in equilibrium with the gravitational force. The settling velocity is used to determine the vertical concentration of sediments near the seabed [25]. It exist several methods, based on the flows Reynolds number, to calculate the settling velocity. The Reynolds number *Re* for a single sand grain is [18]

$$Re = \frac{\omega_s d}{\nu} \tag{89}$$

where ω_s is the settling velocity, d is the diameter of the grain and ν is the kinematic viscosity.

For laminar flows with $Re < 1$, Stokes' law can be applied. Stokes' law describe the drag force F_d exerted on spherical objects viscous fluid [19]

$$F_d = 3\pi\mu D\omega_s \tag{90}$$

where μ is the dynamic viscosity, D is the grain diameter and ω_s is the settling velocity.

The expression of the settling velocity ω_s when Stokes' law is applied, is derived by Lamb in [27]

$$\omega_s = \frac{(\rho_p - \rho_f)}{18\mu} g d^2 \tag{91}$$

where ρ_p is density of the particles, ρ_f is the density of the fluid, μ is the dynamic viscosity, g is the acceleration of gravity and d is the grain diameter.

In [18], Fredsoe and Deigaard derive the following expression for the settling velocity ω_s that can be used for turbulent flow with high Reynolds number

$$\omega_s = \sqrt{\frac{4(s-1)gd}{3c_D}} \tag{92}$$

with

$$s = \frac{\gamma_s}{\gamma} \tag{93}$$

where s is the relative density of the sediment, g is the acceleration of gravity, d is the grain diameter, c_D is the drag coefficient, γ_s is the specific gravity of the sediment and γ is the specific gravity of the fluid.

The relative density s of natural sediments is in most cases in coastal engineering approximated to 2.65. For sand grains, the drag coefficient c_D in a flow with Reynolds number Re is approximately [18]

$$c_D = 1.4 + \frac{36}{Re} \tag{94}$$

Hence, the settling velocity ω_s can be solved analytically by inserting the relation from equation (94) in equation (92).

3.5.2 Sediment distribution in oscillatory flow

The waves at the West Nile Delta represent an oscillatory flow over the plane seabed. Hence, the flow is unsteady and the sediment distribution is given by the following continuity equation [18]

$$\frac{dc}{dt} = \omega_s \frac{\partial c}{\partial z} + \frac{\partial}{\partial z}\left(\varepsilon_s \frac{\partial c}{\partial z}\right) + \frac{\partial}{\partial x}\left(\varepsilon_s \frac{\partial c}{\partial x}\right) \tag{95}$$

where c is the sediment concentration, t is time, ω_s is the settling velocity, z is the vertical coordinate referenced to the seabed, ε_s is the sediment's turbulent diffusion coefficient and x is the horizontal coordinate.

The horizontal concentration gradient is small compared to the vertical concentration gradient. Therefore, the last term in equation (95) can be neglected. Terms related to

convection are of higher order can also be neglected. In [18], Fredsoe and Deigaard use these assumptions to reduced equation (95) to

$$\frac{\partial c}{\partial t} = \omega_s \frac{\partial c}{\partial z} + \frac{\partial}{\partial z}\left(\varepsilon_s \frac{\partial c}{\partial z}\right) \tag{96}$$

where c is the sediment concentration, t is time, ω_s is the settling velocity, z is the vertical coordinate referenced to the seabed and ε_s is the sediment's turbulent diffusion coefficient.

Equation (96) describes the distribution of suspended sediment. Several formulations for the sediment turbulent diffusion ε_s have been developed. Deigaard gives in [28] a detailed description of the turbulent diffusion coefficient ε_s for sediments.

4. Results

4.1 Particle velocity

The horizontal particle velocity is calculated by equation (10) in Airy theory, equation (22) in 2nd order Stokes theory and by using equation (32) with values from Table 4 and Table 5 in the stream function theory. Table 7 contains calculations of the maximum horizontal particle velocity 0.5 m above the seabed using these three theories.

Water depth [m]	Airy theory [m/s]	Stokes 2nd order theory [m/s]	Stream function theory [m/s]
10	1.5914	2.9427	3.1464
15	2.0874	3.5731	3.5757
25	1.8976	2.4593	3.8764
35	1.4530	1.6079	3.2184
50	1.0436	1.0817	2.2961

Table 7: Maximum horizontal particle velocity in [m/s] at different water depths using Airy theory, Stokes 2nd order theory and stream function theory.

The vertical particle velocity 0.5 m above the seabed is calculated by equation (11) in Airy theory, equation (23) in 2nd order Stokes theory and by using equation (33) in the stream function theory. The maximum vertical particle velocity is shown in Table 8.

Water depth [m]	Airy theory [m/s]	Stokes 2nd order theory [m/s]	Stream function theory [m/s]
10	0.0828	0.2016	0.0836
15	0.0813	0.1763	0.0720
25	0.0566	0.0780	0.0552
35	0.0400	0.0431	0.0426
50	0.0252	0.0255	0.0243

Table 8: Maximum vertical particle velocity in [m/s] at different water depths using Airy theory, Stokes 2nd order theory and stream function theory.

4.2 Boundary layer effects

Stokes oscillating boundary layer with variable viscosity is given in equation (73). The real part of equation (73) is solved numerically using the approximated viscosity function given in equation (79) for different values of the coefficient *A.* Figure 10 shows a snapshot of how the dimensionless horizontal velocity amplitude U^* varies with dimensionless distance Z from the moving boundary

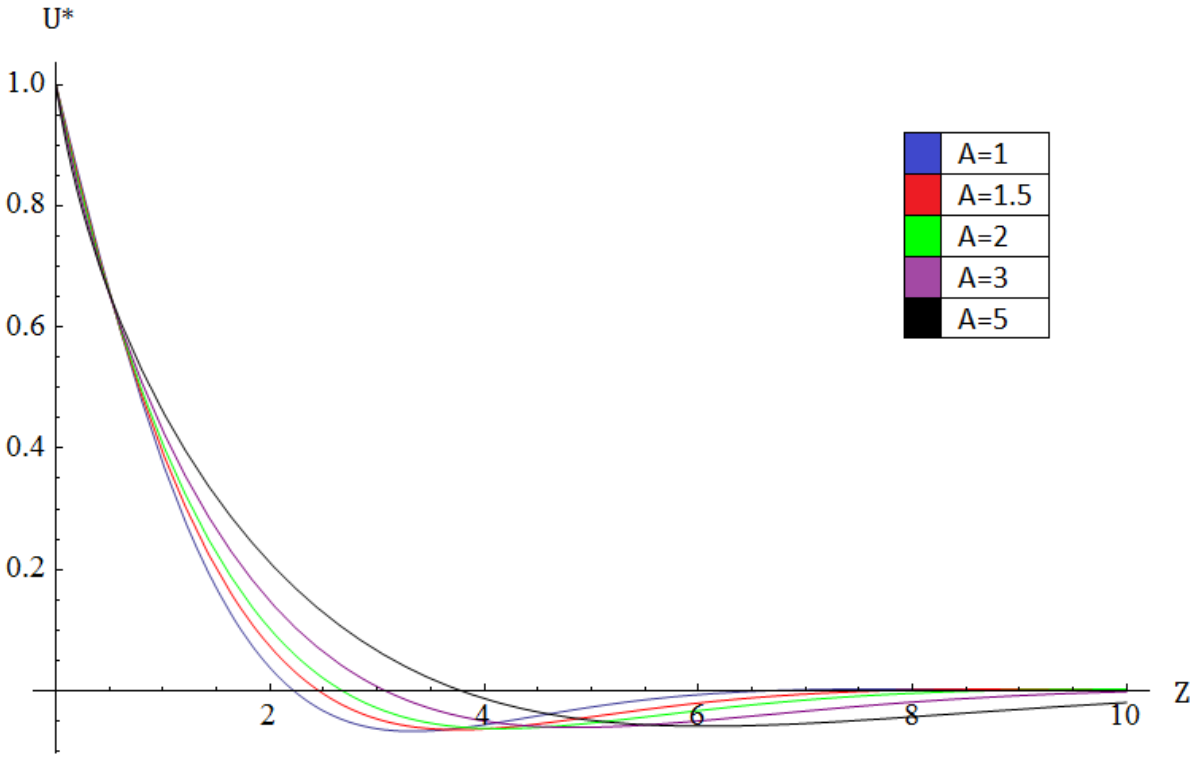

Figure 10: Solution to the real part of Stokes oscillating boundary layer with variable viscosity for different values of the coefficient A.

The imaginary part of equation (73) is also solved, and Figure 11 shows a snapshot of how the dimensionless horizontal velocity amplitude U^* in this case varies with dimensionless distance Z from the moving boundary. The coefficient A is used in the Padé approximation of the variable viscosity.

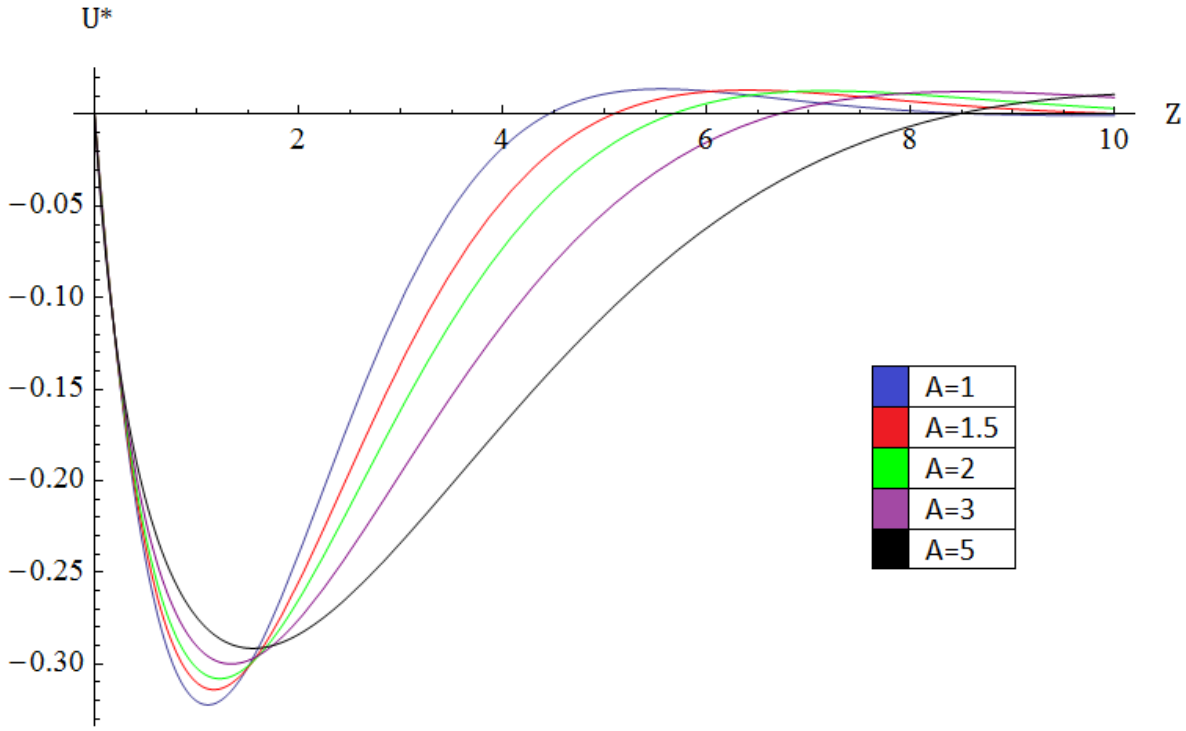

Figure 11: Solution to the imaginary part of Stokes oscillating boundary layer with variable viscosity for different values of the coefficient A.

In section 3.3.4 Dimensionless description of Stokes boundary layera dimensionless description of Stokes boundary layer is derived. Figure 12 is a phase diagram of the dimensionless displacement function X and the dimensionless horizontal velocity u at $t = 0$ for different values of the coefficient A.

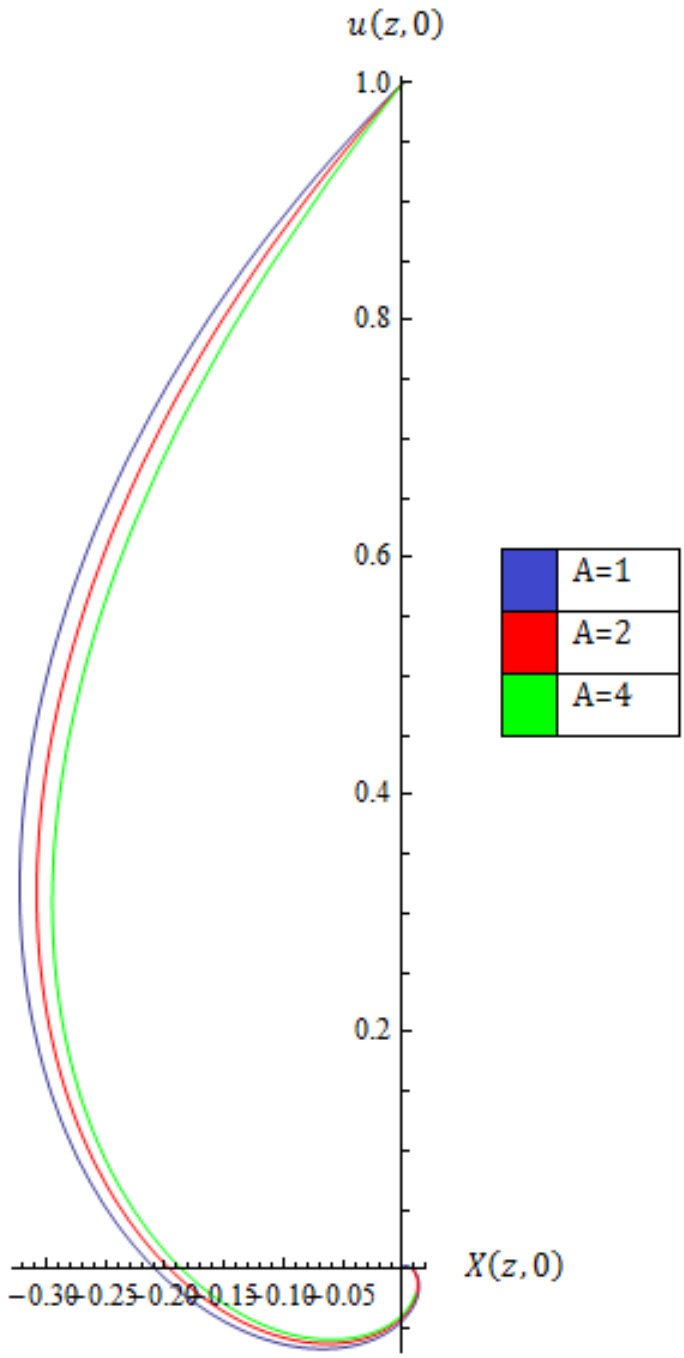

Figure 12: Phase diagram of the dimensionless displacement and the dimensionless velocity. *A* is the coefficient used in the approximation of the variable viscosity.

The plots in Figure 10 and Figure 11 are snapshots of the dimensionless horizontal velocity amplitude. Hence, they are independent of the time *t*. The 3D plots in Figure 13, Figure 14 and Figure 15 represents the complete dimensionless solution of equation (73) with time dependency, for different values of the coefficient *A* used in the viscosity approximations.

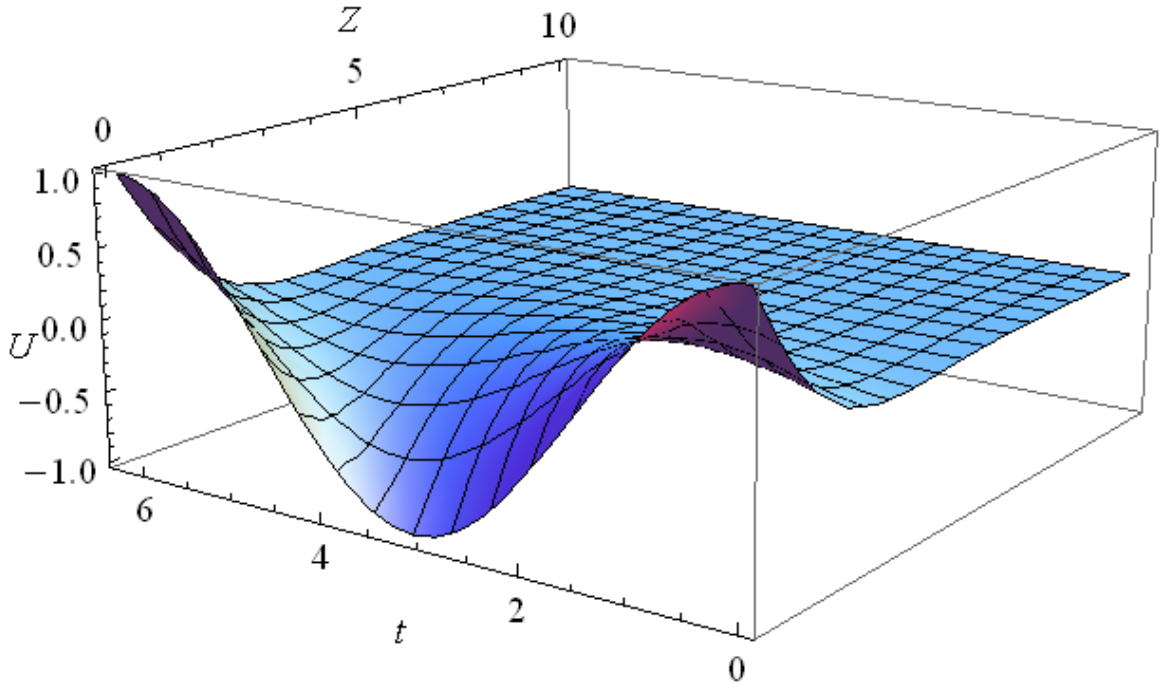

Figure 13: Solution to Stokes oscillating boundary layer with variable viscosity for *A*=1.

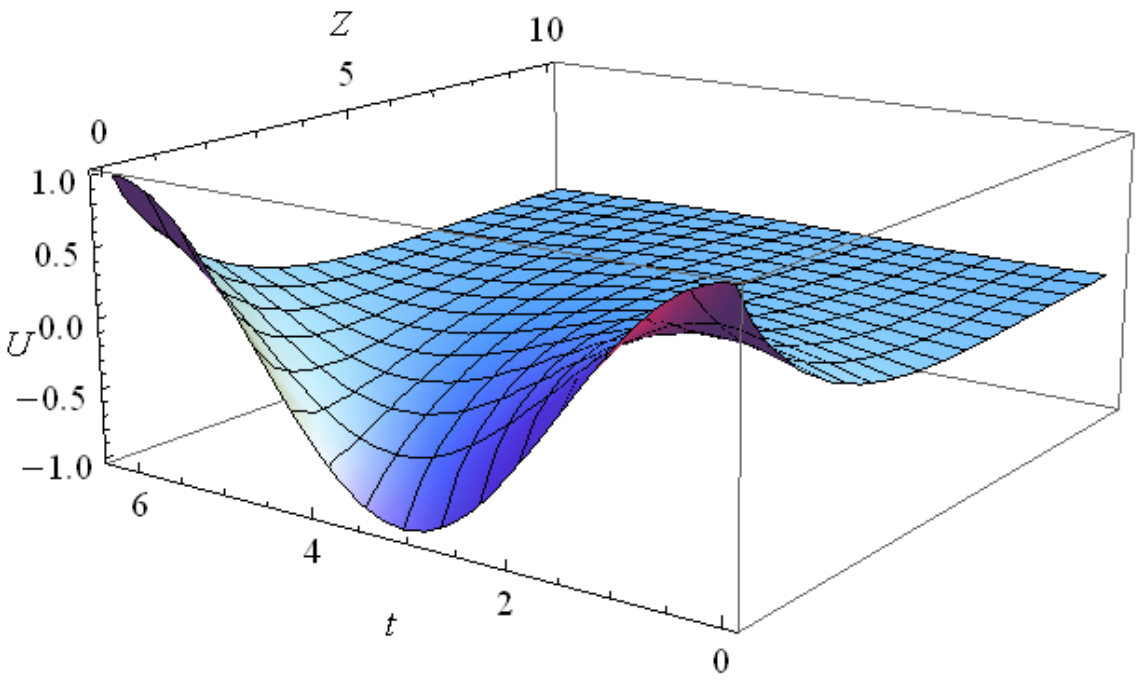

Figure 14: Solution to Stokes oscillating boundary layer with variable viscosity for *A*=4.

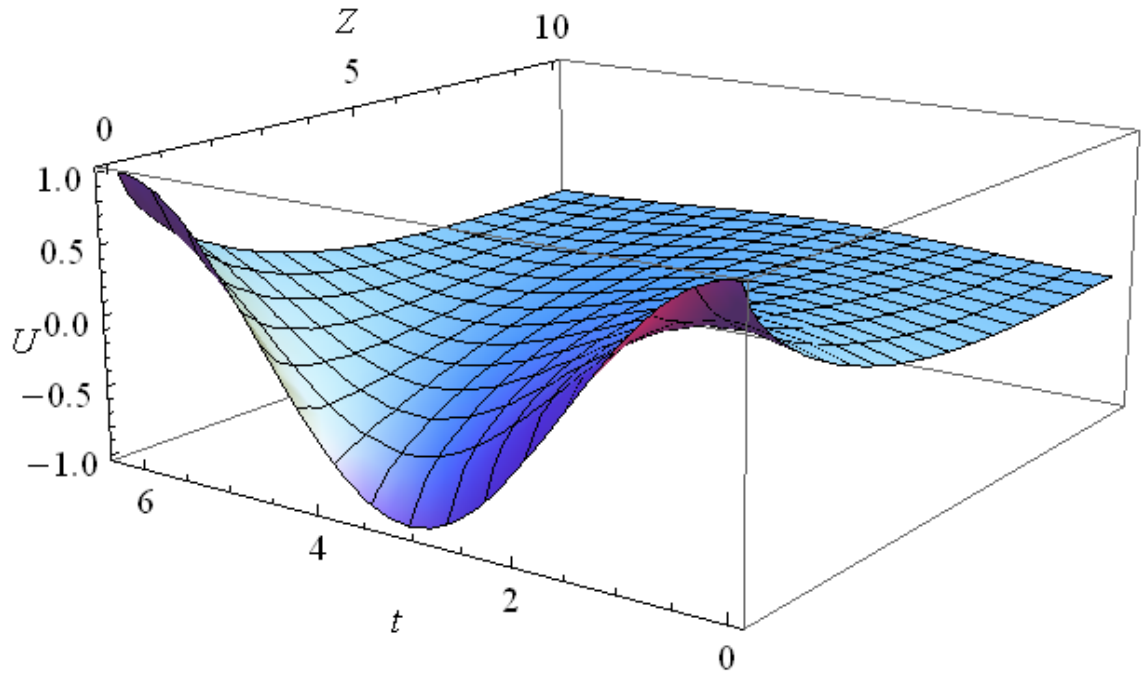

Figure 15: Solution to Stokes oscillating boundary layer with variable viscosity for *A*=8.

5. Discussion

5.1 Wave theory

Horizontal particle velocity

For the maximum horizontal particle velocity listed in Table 7, there were significant differences between the Airy theory and stream function theory in the calculations throughout the depth range. The results indicate that the Airy theory underestimate the values for the maximum horizontal particle velocity for the West Nile Delta case. Stokes 2nd order theory provides good approximations for 10 and 15 meter water depths. For deeper water depths, approximations from the 2nd order stokes theory are significant smaller than the values from the stream function theory.

It is not surprising that the Airy theory does not give an accurate estimate of the horizontal particle velocity. The steepness and shallowness parameters are plotted in Figure 5 to check the validity of different wave theories. The metocean data from the West Nile Delta are far outside of the validity range for the Airy theory. The Airy theory is valid at transitional water depths, but the wave steepness makes the Airy theory invalid for this case. In the Airy theory, the waves are assumed to be symmetrical about the still water level. Hence, the crest and through are assumed to be equal in distance from the still water level. The waves at the West Nile Delta have shown to have steeper and higher wave crests than wave throughs. The surface elevation profile is therefore expected to be inaccurate. This also results in different estimates for the wavelengths between Airy theory and numerical stream function theory. The wavelengths are listed in Table 6. As for the horizontal particle velocity, the Airy theory predicts lower wavelengths than the stream function theory. The differences are largest for the shallowest part of the water depth range. This is also where the differences in approximated maximum velocity are the largest.

The approximations of the horizontal particle velocity from the stream function theory have a high order of accuracy. The stream function satisfies exactly the Laplace Equation, the Bottom Boundary Condition and the Kinematic Free Surface Boundary Condition. Hence, the stream function error is connected to the Dynamic Free Surface Boundary Condition. This boundary condition is satisfied by numerical iteration. DNV

claims in [10], that if the stream function theory is applied correctly, the total error in calculation of the maximum particle velocity is less than 1 %. In the calculations of the maximum particle velocity using the stream function theory, tabulated values for the stream function coefficients and the stream function wave length was used. These values were extracted from [17] by interpolation of relevant cases. Some error is expected to be connected with the accuracy in the interpolation.

Vertical particle velocity

Both the Airy theory and the stream function theory predicted the maximum vertical particle velocity to be close to zero. The results were almost identical for both theories, as shown in Table 8. From a wave theory stand point, this is as expected.

The 2nd order Stokes theory approximates significantly higher vertical velocity at 10 and 15 meters water depth. The values are still close to zero and small compared to the horizontal velocity at the same water depths. Notice, that the 2nd order Stokes theory provides best approximations of the horizontal particle velocity and worst approximations of the vertical particle velocity at 10 and 15 meter water depths at the West Nile Delta.

5.2 Boundary layer effects on the horizontal particle velocity

The Stokes oscillating boundary layer with variable viscosity problem, equation (73), is solved numerically to evaluate boundary layer effects on the wave flow. Figure 10, Figure 11, Figure 13, Figure 14 and Figure 15 show how the dimensionless velocity amplitude varies with the dimensionless distance, for different approximates of the variable viscosity. The shape of the velocity profile clearly indicates that the boundary layer affect the oscillating wave flow. If the boundary layer was neglected, the velocity profile near the boundary will be straight vertical lines with reversing paths.

The variable viscosity is empirically approximated using Padé approximant. The viscosity function should vary monotonically with the distance and have a finite value when the distance goes to infinity. Padé approximant is one of the easiest ways to approximate such function and is therefore used in the approximations. Taylor series could not be used in this case, because the solution will diverge to infinity.

The coefficient A is used to approximate the variable viscosity. By increasing this coefficient, the boundary layer thickness increases. This is because the shear stress increases for larger values of the coefficient A, with the distance from the moving boundary. For high values of the coefficient A, the boundary layer becomes so thick that the non-linear term $u\frac{\partial u}{\partial x}$ in the Navier-Stokes equation must be taken into account.

The approach of solving Stokes boundary layer with variable viscosity is inconsistent in an energy aspect. The boundary layer causes viscous loss of mechanical energy. This energy must be taken from somewhere, and the most natural is that the wave amplitude decreases with time. This loss in mechanical energy is not accounted for in the thesis. This inconsistency may be fixed by writing the solution as an asymptotic development in powers of the viscosity, and then the following term in the power series is a correction to the inconsistency.

6. Conclusion

The results in this master thesis show that the intermediate Airy theory significantly under-predicts the horizontal particle velocity close to the seabed for the West Nile Delta case. Hence, the Airy theory is not applicable for steep water waves in shallow and transitional water depths. The calculations also shows that Stokes 2nd order wave theory overall provides better results than the Airy theory, especially for the shallowest water depths. Nevertheless, the results obtained by using 2nd order Stokes wave theory is not satisfying over the whole water depth range. In calculations of environmental loads on submerged structures in shallow and transitional water depths, the stream function theory gives accurate approximations of the wave kinematics and should be applied.

The evaluation of boundary layer effects on the oscillating wave flow close to the seabed indicates that the boundary layer will affect the velocity profile near the boundary. The results from the Stokes boundary layer theory with variable viscosity shows that boundary layer thickness grows with increasing approximates for the viscosity. This is due to increased shear stress acting on the oscillating flow.

6.1 Further work

In the calculations of horizontal velocity using Airy theory, 2nd order Stokes theory and stream function theory, the water current was neglected. Further development of the wave theories could include the effects of currents on the horizontal velocity. By including effects of currents, a more complete solution to the wave kinematics may be obtained.

The evaluation of the boundary layer effects in this thesis neglect sediment transport in the boundary layer. Further work is recommended to include effects of sediment transport on the wave flow in the boundary layer near the seabed.

Bibliography

1. **Nexans Norway AS.** Nexans in Norway. [Online] Nexans. [Cited: 23 April 2013.] http://www.nexans.no/eservice/navigation/NavigationPublication.nx?navigationId=217577.

2. **Gjevik, Bjørn, Pedersen, Geir K and Trulsen, Karsten.** *Forelesninger i bølgeteori.* Oslo : Matematisk institutt, Universitetet i Oslo, 2007.

3. **Olsen, Margaret.** SECOORA. *Waves Glossary.* [Online] Southeast Coastal Ocean Observing Regional Assosiation. [Cited: 14 February 2013.] http://secoora.org/classroom/virtual_wave/glossary.

4. **Journèe, Johan M. J. and Massie, W. W.** *Offshore Hydrodynamics.* Delft : Delft University of Technology, 2001.

5. **Newman, John Nicholas.** *Marine Hydrodynamics.* Cambridge : The MIT Press, 1977.

6. **Sorensen, Robert M.** *Basic Coastal Engineering.* 3. New York : Springer Science + Business Media, Inc, 2006.

7. **The 1911 Classic Encyclopedia.** Sir George Biddell Airy. [Online] The 1911 Classic Encyclopedia. [Cited: 14 February 2013.] http://www.1911encyclopedia.org/Sir_George_Biddell_Airy.

8. **PDHengineer.com.** *Coastal Engineering - Water Wave Mechanics.* Houston, TX : PDHengineer.com, 2008.

9. **Hu, James.** *Marine Structure Designs, Lecture #2.* Rhode Island, RI : The University of Rhode Island, 2003.

10. **DNV.** *Environmental Conditions and Environmental loads.* 2010.

11. **Holmes, patrick.** *Coastal Processes: Waves.* London, UK : Imperial College, 2001.

12. **DNV.** About us: DNV. *Company Profile.* [Online] [Cited: 18 February 2013.] http://www.dnv.com/moreondnv/profile/about_us/.

13. **Chakrabarti, Subrata Kumar.** *Hydrodynamics of Offshore Structures.* Southampton : WIT Press, 1987.

14. **Dean, R. G.** *Evaluation And Development Of Water Wave Theories For Engineering Application, VOL. 1.* Fort Belvoir, VA : U.S. Army Coastal Engineering Research Center, 1974.

15. **Rienecker, M. M. and Fenton, J. D.** *A Fourier approximation method for steady water waves.* Cambridge, UK : Cambridge University Press, 1981.

16. **Svendsen, Ib A.** *Introduction To Nearshore Hydrodynamics.* Singapore : World Scientific Publishing, 2006.
17. **Dean, R. G.** *Evaluation And Development Of Water Wave Theories For engineering Application, VOL. 2.* For Belvoir, VA : U. S. Army Coastal Engineering Research Center, 1974.
18. **Fredsøe, Jørgen and Deigaard, Rolf.** *Mechanics of Coastal Sediment Transport.* Singapore : World Scientific Publishing Co. Pte. Ltd., 1992.
19. **Batchelor, G. K.** *An Introduction to Fluid Dynamics.* Cambridge : Cambridge University Press, 1967.
20. **Encyclopædia Britannica.** Britannica. *Sir George Gabrial Stokes, 1st Baronet.* [Online] Encyclopædia Britannica, Inc. [Cited: 3 April 2013.] http://www.britannica.com/EBchecked/topic/566981/Sir-George-Gabriel-Stokes-1st-Baronet.
21. **Finnemore, E. John and Franzini, Joseph B.** *Fluid Mechanics with Engineering Application.* Singapore : McGraw-Hill, 2009.
22. **Durbin, P. A. and Reif, B. A. Petterson.** *Statistical Theory and Modeling for Turbulent Flows.* Chichester : John Wiley & Sons Ltd, 2001.
23. **Wolfram Mathworld.** Taylor series. *Wolfram Mathworld.* [Online] [Cited: 3 May 2013.] http://mathworld.wolfram.com/TaylorSeries.html.
24. **Wolfram Mathworld.** Rational function. *Wolfram Mathworld.* [Online] [Cited: 2 May 2013.] http://mathworld.wolfram.com/RationalFunction.html.
25. **Amoudry, Laurent.** *A Review on Coastal Sediment Transport Modelling.* Liverpool : Proudman Oceanographic Laboratory, 2008.
26. **Navarro, Pilar Garcia and playan, Enrique.** *Numerical Modelling of Hydrodynamics for Water Resources.* Zaragoza : Taylor & Francis, 2007.
27. **Lamb, H.** *Hydrodynamics.* Cambridge : Cambridge University Press, 1932.
28. **Deigaard, Rolf.** *On the Turbulent Diffusion Coefficient for Suspended Sediment.* Lyngby : EV, 1991.